EFFECT OF MANUFACTURING-INDUCED DEFECTS AND ORIENTATION ON THE FAILURE AND FRACTURE MECHANISM OF 3D PRINTED STRUCTURES

By

AMIT KHATRI

Presented to the Faculty of the Graduate School of

The University of Texas at Arlington in Partial Fulfillment

of the Requirements

for the Degree of

MASTER OF SCIENCE IN MECHANICAL ENGINEERING

THE UNIVERSITY OF TEXAS AT ARLINGTON

DECEMBER 2016

ACKNOWLEDGEMENTS

First of all, I would like to express my deepest gratitude to my advisor Dr. Ashfaq Adnan, for his patience, support, valuable guidance and encouragement through the entire journey of my thesis completion every step on my way. I wish to thank him for providing me with all the necessary facilities for the research. I am extremely fortunate to have an advisor like him. In addition to guiding through my research, he respected, believed in me, treated as a family and took responsibility to shape my personality.

I would like to thank Stratasys/America Makes for all funding and support provided for this research work. I am also thankful to Mr. Brian Shonkwiler for his valuable help with the instruments during experiments and special thanks to Dr. Andrew Makeev for letting us use their facilities. I would like to thank the members of my doctoral committee, Dr. Wen S. Chan, Dr. Robert Taylor for their valuable discussions and accessibility. I would like to thank the department of Mechanical and Aerospace Engineering at UTA, especially Dr. Seiichi Nomura for being a wonderful graduate advisor. I am also grateful to the following staff at The University of Texas at Arlington, for their various forms of support during my graduate study—Debi Barton, Lanie Gordon, Louella Carpenter, Sally Thompson and Catherine Gruebbel.

I wish to express special thanks to all my colleagues- Ferdous, Sheikh F , Manikanta Jonnalagadda, Peter Louis Deboullac, Sheikh Fahad Ferdous, Issac Blesson, Sachin Jose, Saketh Thappliyal, Riaz Kaiser for their support, guidance and valuable suggestions. Most importantly, I wish to express my sincere gratitude to my parents who always believed in me and made me the person that I am today. They gave me love, support and strength through all good and bad days of my life.

December 11, 2016

ABSTRACT

EFFECT OF MANUFACTURING-INDUCED DEFECTS AND ORIENTATION ON THE FAILURE AND FRACTURE MECHANISM OF 3D PRINTED STRUCTURES

Amit Khatri, M.S.

The University of Texas at Arlington, 2016

Supervising Professor: Ashfaq Adnan

Additive manufacturing is a rapidly growing cutting edge technology. Number of experimental studies have shown that strength of product manufactured by additive Fused Deposition Method (FDM) is influenced by different processing parameters involved during manufacturing. This thesis work presents experimental and theoretical investigation of mechanical behavior of ABS material fabricated with variation in some of process parameters such as Axis Orientations, Raster Orientation, Infill Percentage, Layer Height and Number of Shells. Different experiments were designed to understand the basics of 3D printing manufacturing and to characterize the mechanical behavior of 3D printed structures. This study helps to understand, how different raster orientations affects the fracture toughness of 3D printed structures and also tell us under which process parameters additive manufactured structures provide better tensile, shear and compressive strength. Using this study we can understand and develop optimized manufacturing process for robust 3D printing manufacturing.

Table of Contents

List of Illustrations

List of Tables

Chapter 1

INTRODUCTION

Recent developments in additive manufacturing (also known as 3D Printing) provided a tool to design and create complex structures in a short period of a time. Additive Manufacturing has covered most of the technologies with varying advantages and disadvantages. Medical, Automotive and Aerospace are of most rapidly growing sectors in Additive Manufacturing among all others. The main reason behind is additive manufacturing allows for cheap, low-volume production and facilitates personalized and customized products. Besides all advantages, several fundamental challenges such as developing standards, improving material affordability, and increasing the reliability and accuracy of equipment need to be addressed. Therefore, industrialized economies are working to develop and strengthen productivity and competitiveness of additive manufacturing.

The aim of the study is to develop understanding of Fused Deposition Method (FDM) for producing and manufacturing end use products by evaluating mechanical characteristics of 3D printed structures and materials. To make it more precise, the study basically focuses on few important questions such as,

- What all factors affect 3D printed structures? How does they affect manufacturing process?
- Is it possible to predict mechanical behavior of 3D printed structures?
- Does 3D printed structures behave similar way for all different manufacturing methods?
- Is it possible to replace traditional manufacturing methods by 3D printing manufacturing?

Therefore in this research study we tried to experimentally investigate the mechanical behavior of 3D printed ABS material by completing Tensile, Shear and Compressive testing using ASTM standards.

Chapter 2

LITERATURE SURVEY

Okwara et al. [1] studied behavior of 3D printed structures under different raster orientations and mentioned that structural strength is maximum when fibers are aligned along the tensile force direction. Montero et al. [2] experimented on effect of surrounding temperature, fiber width, and air gap and raster orientation under compressive and tensile loading conditions. This study evaluated that raster orientation and gaps between layers affected the tensile strengths of the structure but there was least impact on compressive strength. Similar study was developed by Sun et al. [3] where they studied behavior under variation of build directions, raster orientation, layer thickness and width. They developed relationship between different process parameters and tensile strength of ABS material. This study has been further developed for other loading conditions such as compressive, bending and shear loading. All these studies shows results that describe the importance of bond strength among the layers and effect of raster orientation on the FDM structures.

Research done by Sharma et al. [4] explored effect of raster orientation on tensile and fatigue loading conditions. They concluded that unidirectional fibers along the tensile force direction shows the highest tensile strength while alternating lamina with orientation -45°/+45° represents maximum fatigue strength. Huang et al. [5] also studied behavior of ABS material under tensile and compressive loading conditions and characterized the properties under different parametric conditions. They concluded that ABS material gets affected more under tensile loading due to orientations and gaps between layers.

All these studies made it easy to understand in fused deposition modeling structural strength is dependent on various parameters involved in manufacturing. So the work represented in this paper investigates further the fracture mechanics of the additive manufactured ABS material manufactured under varying processing parameters.

Chapter 3

ADDITIVE MANUFACTURING / 3D PRINTING

3.1 What is 3D Printing?

3sD printing is a type of additive manufacturing process where objects are manufactured from digital file. In additive manufacturing product is developed from bonding of succeeding material layers. For developing a product it is required to have a digital 3-D model. We can scan any objects or draw complete 2D drawing using CAD software. The file is saved in STL format and then the process of printing product layer by layer is started.

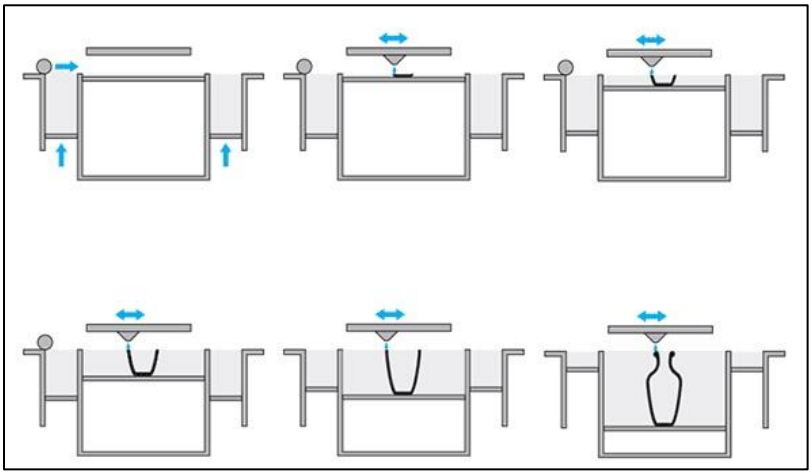

Figure 3 -1 3D Printing Method [6]

Additive manufacturing / 3D printing is one of the game changing technology which can manufacture parts from scratch in very short period of a time and also saves material cost. It gives all freedom to designers to develop a design without any constraints of manufacturing as compared to traditional manufacturing methods. Today almost every field is using 3D printing manufacturing from toys to aerospace because 3D printing is saving big amount on assembling products as it can directly print assembled products. 3D printing is allowing all industries to make number of trials on prototyping and make changes to the design for the best fit. And the best part is it is not consuming extra time or cost for the manufacturing. 3D printing made prototyping much faster that is why it is also known as '**Rapid Prototyping**'.

3.2 How does 3D Printing Works?

Basically 3D printing process starts from the CAD design of the parts. Once the parts are designed using CAD tools, they are sliced into number of layers using 3D printing software. Software not just helps to divide designed part into layers but also provides accessibility to decide processing parameters for the manufacturing. Software stores file in STL format and that is an input file for the 3D printer.

In 3D printing the material spool of long filament is attached to the 3D printing machine. The 3D printing machine also controls the temperature of the extruder and platform. Once the extruder reached to the melting temperature of material, the material is passed through the extruders using control system worked by servo motors. The Extruder melts the material and allow it to flow through the nozzle to the platform. Printers are designed to follow the input design using the electronic controllers. Using this method first layer get printed on the platform and then same process is getting repeated for each and every layer as shown in Figure 2. This way 3D printing gives a freedom to manufacture most of the complicated design in an easy manner with a low cost. That is one of the major reason behind rapid studies continuing in the field of additive manufacturing.

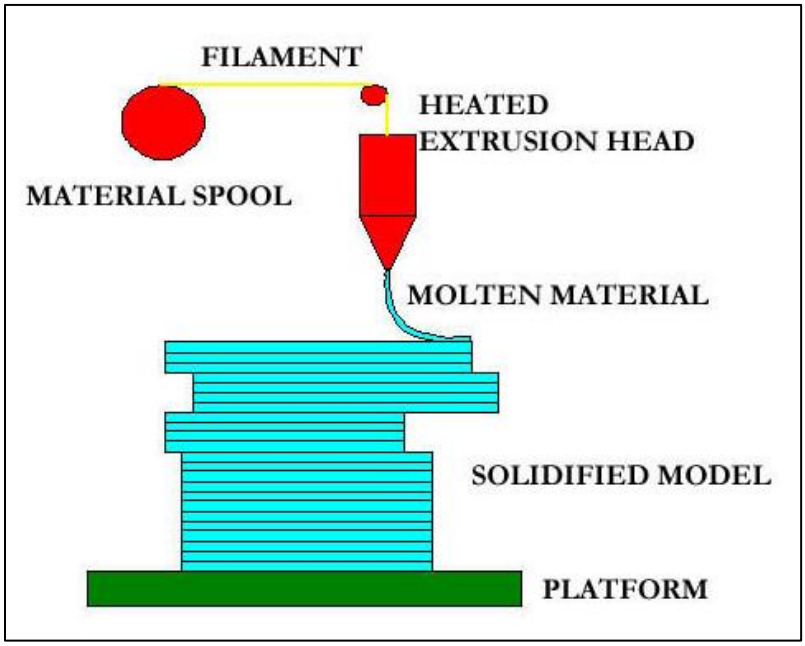

Figure 3 -2 Fused Deposition Modeling [7]

3.3 Types of 3D Printing

Today many different types of additive manufacturing processes are available in the market. The basic difference between several processes is in the material to be used and the method used for manufacturing layer by layer. Few methods deposit layer by melting the material over bed, while other methods solidifies liquid or powder form of material layer by layer using advanced technologies like laser beam. In following table we can see all different types of 3D printing technologies and materials used for them.

Table 3-1 Types of 3D Printing [8]

TYPE	TECHNOLOGIES	MATERIALS
EXTRUSION	Fused deposition modelling (FDM) or Fused filament fabrication (FFF)	Thermoplastics, eutectic metals, edible materials, Rubbers, Modelling clay, Plasticine, Metal clay (including Precious Metal Clay)
	Robocasting or Direct Ink Writing (DIW)	Ceramic materials, Metal alloy, cermet, metal matrix composite, ceramic matrix composite
LIGHT POLYMERIZED	Stereolithography (SLA)	Photopolymer
	Digital Light Processing (DLP)	Photopolymer
POWDER BED	Powder bed and inkjet head 3D printing (3DP)	Almost any metal alloy, powdered polymers, Plaster
	Electron-beam melting (EBM)	Almost any metal alloy including Titanium alloys
	Selective laser melting (SLM)	Titanium alloys, Cobalt Chrome alloys, Stainless Steel, Aluminium
	Selective heat sintering (SHS)[44]	Thermoplastic powder
	Selective laser sintering (SLS)	Thermoplastics, metal powders, ceramic powders
	Direct metal laser sintering (DMLS)	Almost any metal alloy
LAMINATED	Laminated object manufacturing (LOM)	Paper, metal foil, plastic film
POWDER FED	Directed Energy Deposition	Almost any metal alloy

3.4 Advantages of 3D Printing

Additive manufacturing's particular technique and various types has stepped up in the competitive world by opening doors for innovations and it offers wide range of strategic, profitable and technical benefits. In this section we will discuss some of the advantages in brief:

3.4.1 Low Cost Manufacturing :

Additive manufacturing becomes cheaper as it works with limited material and uses less human resources for manufacturing. As compared to traditional manufacturing 3D printing saves many steps involved in manufacturing, assembling and finishing of the product. Therefore it is the most reasonable factor for industries to get involved in 3D printing.

3.4.2 Rapid Production:

Speed of 3D printing manufacturing is many times faster as compared to traditional manufacturing processes. Now parts can be manufactured in few hours where old methods were used to take several days. 3D printing machines can run overnight which gives an advantage of 24 hours manufacturing without labor cost. Therefore additive manufacturing developed on demand manufacturing pattern due to which industries do not need to manufacture all products in advance. That again saves cost of storage and required processing.

3.4.3 Material Saving:

Manufacturing components using metals or plastics using traditional methods like CNC, molding etc. used to create lots of waste material at the end of process. In aircraft or auto parts manufacturing most of the material got used to waste because of very particular design specifications. On the other side using 3D printing, similar parts can be manufactured using minimum material. As no extra material is used for manufacturing in 3D printing, minimum waste is created which saves lot of material for manufacturing. And indirectly that saves the final cost of manufacturing. Also waste has a great impact on the environment. Therefore 3D printing also helps to achieve low impact of waste material on an environment.

3.4.4 Freedom for Complex Designs:

Traditional manufacturing methods were basically depended on molding, cutting and CNC manufacturing where most of material was getting subtracted to get the final product. Due to subtractive manufacturing method there was restrictions over design because of which creating a complex design was a great challenge.3D printing changed the game in this area as it can create any design using pointed nozzle tip or laser beam technology. Therefore a designer do not get much constraints for designs which helps to implement innovative ideas easier way. Also 3D printing made it possible to manufacture cellular structures which are most useful in medical and aerospace manufacturing.

3.4.5 Feasibility for New Materials:

Mixing materials using traditional methods of manufacturing was not always easy because of different reasons like cost of raw materials or sometime the processing cost due to physical and chemical properties of the material. 3D printing is eliminating most of this boundaries over materials. In 3D printing it became easier to try new materials by combining different materials together. Many industries became successful to manufacture several plastic materials with feel and look of metals with various strengths. Also there are different biodegradable materials available which can be used for medical industry which are great examples for material success.

3.4.6 Wide range of Applications:

Additive manufacturing is useful in number of different areas of study such as automotive, consumer products, business machines, medical, education, aerospace and many other. This is one of the major advantage of 3D printing as only single machine can manufacture for wide range of applications. This machines are available in all scales which gives advantage to consumers to 3D print products even while sitting at home as it does not necessarily requires particular environment for manufacturing.

Chapter 4

PARAMETERS INFLUENCING 3D PRINTING

4.1 INTRODUCTION

3D printing basically depends on various factors involved in manufacturing. There are different parameters which influences the strength, manufacturing speed and quality of the product. Therefore before getting into depth of 3D printing it is very important to know what all parameters affect 3D printing manufacturing and is there any possible way to control them. The following fishbone diagram gives an overview of all different parameters those affect the mechanical properties of 3D printed structures and materials.

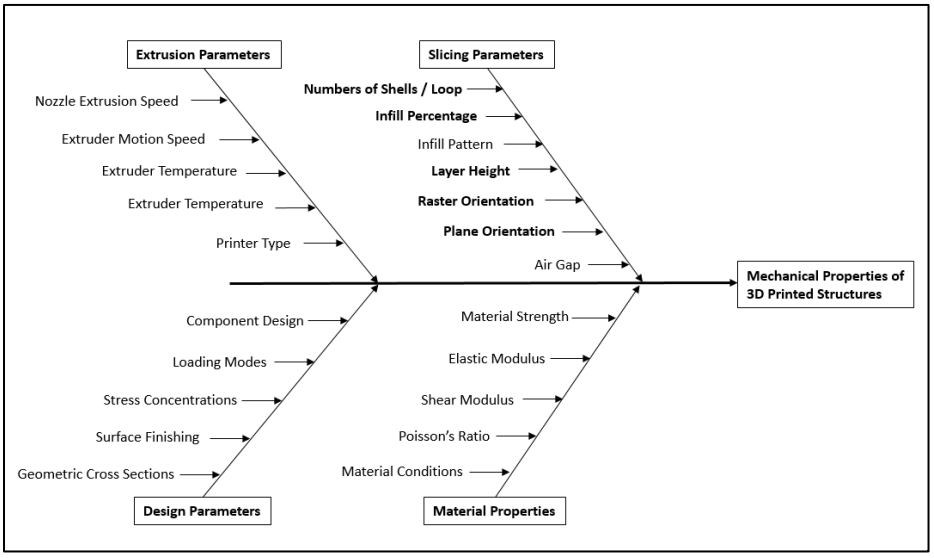

Figure 4-1 Fishbone Diagram of Influential Parameters of 3D Printing [9]

As shown in Figure 4.1, major mechanical properties of 3D printed structures basically depends on four main parameters such as Slicing Parameter, Extrusion Parameter, Design Parameters and Material Properties. In this study we will focus on Slicing parameters which can be controlled using 3D printer software so that it will help in future to understand level of manual control over strength, quality and manufacturing time of 3D printed products. Therefore in this chapter we will study more details of parameters like Number of shells, Infill percentage, Layer height, raster orientation, plane orientation and also discuss in detail quantitative effect of each parameter over the final product.

4.1.1 Infill Percentage:

Infill is amount of material used for the manufacturing whereas the infill percentage is the percentage of the total volume of the material required for the manufacturing.

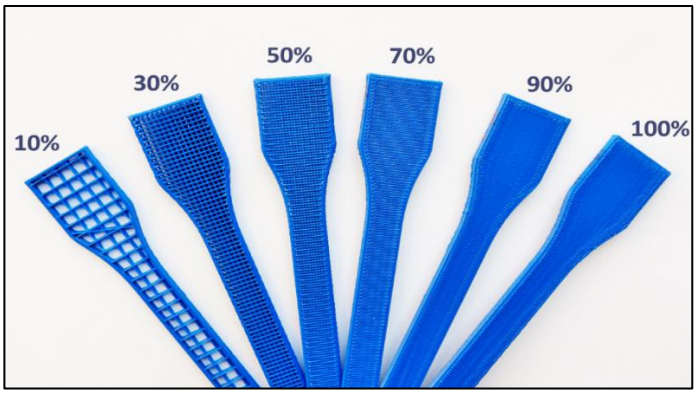

Figure 4-2 Infill Percentage variation [10]

As we can see in Fig. 4-2, as we increase the infill percentage the material used for manufacturing increases and therefore the stiffness of the product. But on the other side it also takes some extra time to manufacture the specimen with extra infill.

4.1.2 Infill Pattern:

In Fused Deposition Methods (FDM), one more advanced option is to control the pattern of infill material which helps to save time and take control over the strength of the structure. Infill pattern is divided in few different types such as Linear, Diagonal, Hexagonal, Moroccan stars, Catfill etc. Figure 4.3 shows exact pattern of each type.

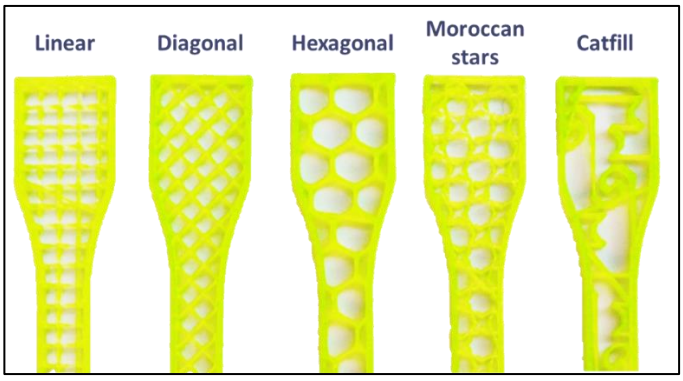

Figure 4-3 Infill Pattern variation [11]

4.1.3 Layer Height:

In additive manufacturing final product is manufactured layer by layer. So there is a good option to decide the height of each layer which is known as Layer Height. Figure 4.4 gives the clear picture of layer height variation. As we increase the layer height it decreases the number of layers which indirectly saves time of manufacturing.

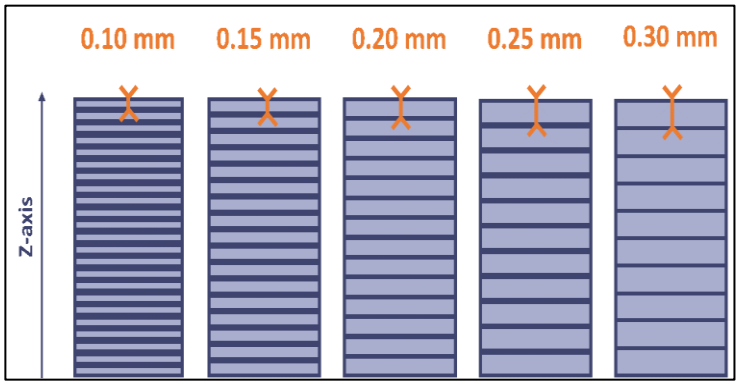

Figure 4-4 Layer Height Variation [12]

4.1.4 Number of Shells / Loops :

Number of shells is the total number of material loops extruder will develop around the perimeter of the 3D printed structure. So basically it is analogous to the wall of a house. As more number of walls gives more safety, similar way more number of shells makes structure stronger towards the external loads. The number of shells tells you how many times extruder nozzle going to run over the perimeter of the structure. But increase in number of shells also increases the time required for manufacturing.

Figure 4-5 Variation in Number of Shells / Loops

4.1.5 Plane Orientation:

3D printing manufacturing can be done in different plane orientations. It can be done in all three planes such as XYZ plane, XZY plane and ZXY plane as shown in Fig.4.6. Therefore it is very important to know in which plane manufacturing can be done easier way to get optimized strength.

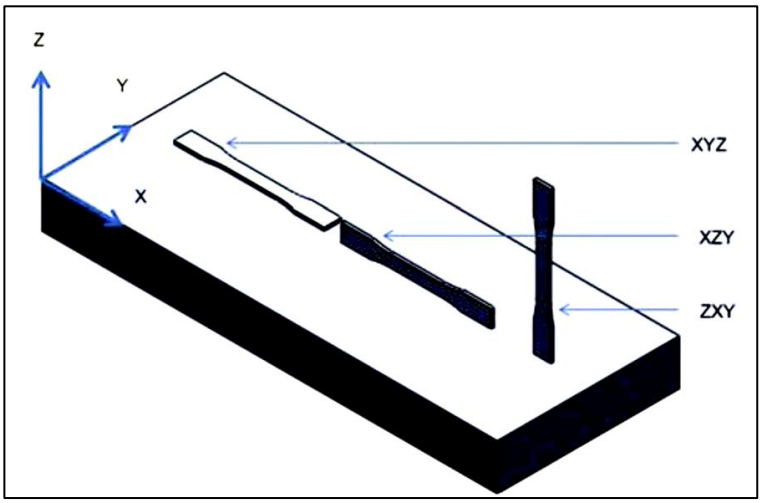

Figure 4-6 Different Plane Orientations

4.1.6 Raster Orientations:

Most interesting part in 3D printing manufacturing is we can decide the direction of manufacturing. So 3D printing machine controls the path of manufacturing and it can be done in various orientations along the plane. This moment of extruder along different angle is known as Raster Orientation as shown in Fig.4.7.

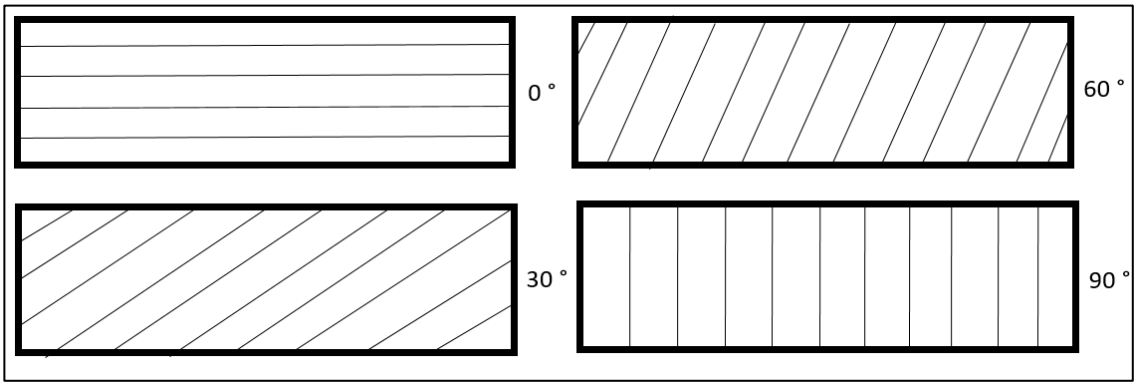

Figure 4-7 Different Raster Orientations

4.2 DESIGN OF EXPERIMENT:

After getting an overview of different parameters influencing 3D Printing, it is very important to understand which parameter affects the most with respect to material strength, finish quality and time for manufacturing. Therefore we have designed an experiment where we manufactured a specimen with different combinations of parameters and completed tensile testing of each specimen. Tensile test data was analyzed to understand the effect of each parameter. More details of experiment are discussed as follow,

4.2.1 Theory :

This experiment is focused on influence of four major parameters; Infill Percentage, Number of shells, Layer Height and plane orientation. These parameters can control the speed and quality of manufacturing and they also affect the strength of the product. Different specimens were designed and manufactured with variation of each parameter. To understand the individual effect of each parameter one parameter was varied at a time that means all other parameters were set to default settings and just one parameter was changed individually. We can understand more details of the experiment in further sections.

4.2.2 Specimen Design and Construction:

For the study of parameters specimens with dimension (80x15x5) mm were designed in CATIA V5 as shown in Fig. 4.8.

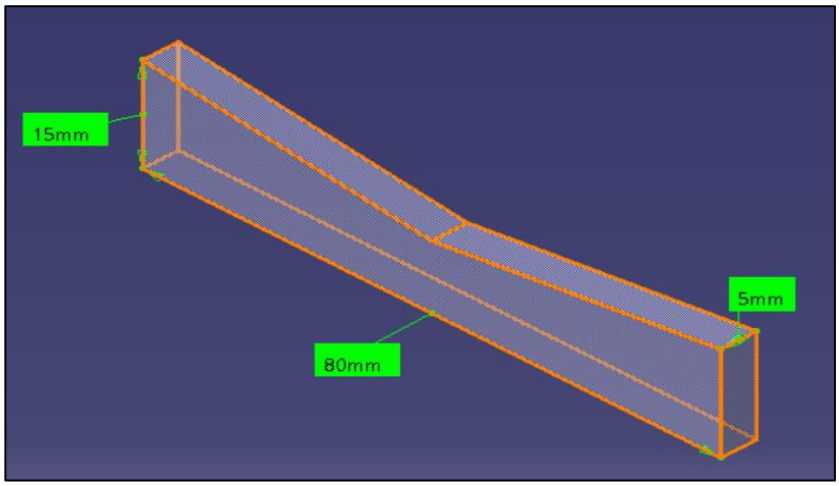

Figure 4-8 Specimen Design for Parameter Analysis

Finalized design was saved as .STL file using CATIA V5 and the same file was used as an input file for slicing software of MAKERBOT 3D printer. In this software all parameters were adjusted as per requirement. So for our study we created 15 different sets of parameters where every parameter was varied in different aspects. The list of all sets of parameters is as given below,

Table 4 - 1. Parameter setting w.r.t. variations

PARAMETERS	INFILL PERCENTAGE	LAYER HEIGHT	NUMBER OF SHELLS	PLANE ORIENTATION
DEFAULT	50%	0.30 mm	1	XZY
INFILL VARIATION	**25%, 50%, 75%, 100%**	0.30 mm	1	XZY
LAYER HEIGHT VARIATION	50%	**0.10mm, 0.15mm, 0.20mm, 0.25mm**	1	XZY
VARIATION IN NUMBER OF SHELLS	50%	0.30 mm	**1, 2, 3, 4**	XZY
VARIATION IN PLANE ORIENTATION	50%	0.30 mm	1	**XYZ, XZY, ZXY**

Once all parameters were set all files were sliced as per settings and saved in .X3G format. Then this file is given as input to the Makerbot Replicator 2X machine. Using this 3D Printers 3 iterations of each specimen were manufactured as shown in Fig.4.9.

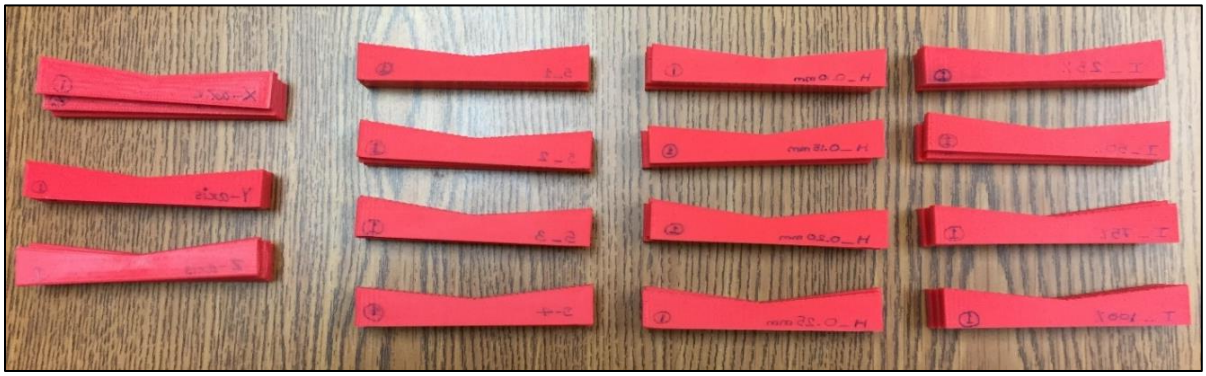

Figure 4-9 3D Printed Specimen for Parameter Testing

4.3 RESULTS

After completion of manufacturing all specimens were tested for tensile loading under Shimadzu Universal testing machine. And all results are tabulated as given below,

4.3.1 Effect of Infill Variation:

From the given bar charts we can observe that variation in infill percentage has high impact on the strength, material quantity and manufacturing time.

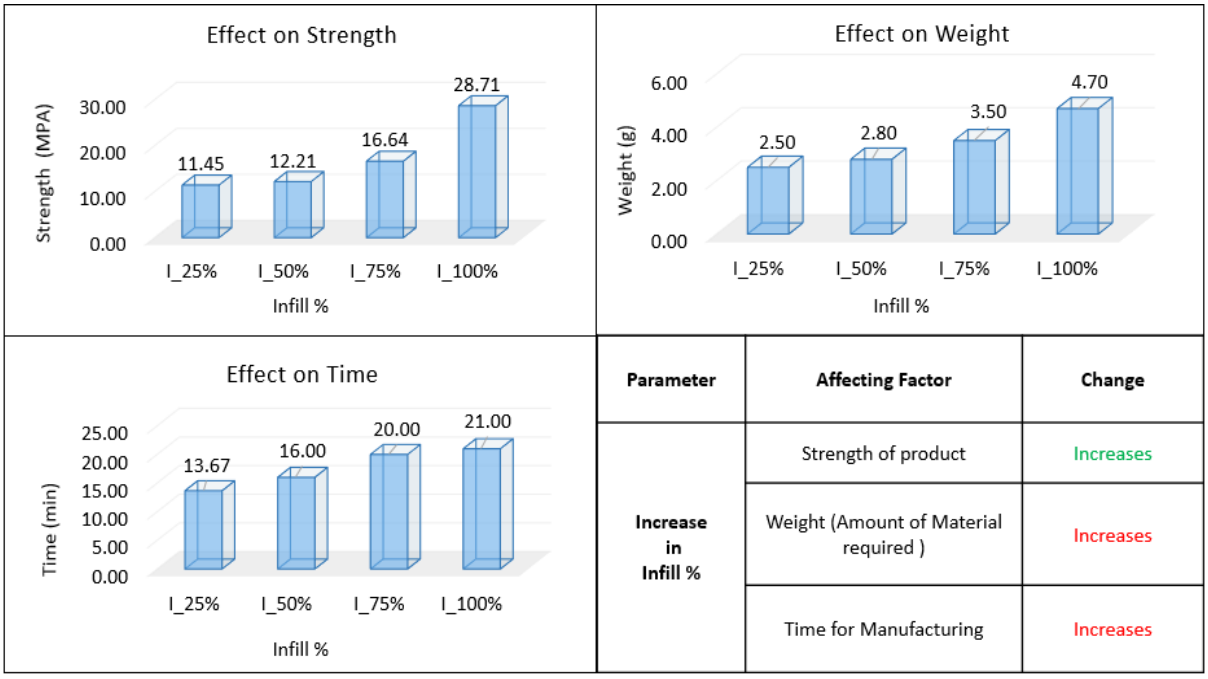

Parameter	Affecting Factor	Change
Increase in Infill %	Strength of product	Increases
	Weight (Amount of Material required)	Increases
	Time for Manufacturing	Increases

Figure 4-10 Effect of Infill % on Tensile Strength, Product Weight and Manufacturing Time

Above graphs give clear picture of behavior of the material with respect to variation in infill percentage. The specimen with 25% infill shows less tensile strength as it uses less material and less time for manufacturing as compared to 50%, 75% and 100% infill specimens. On the other side, specimen with 100% infill shows the highest strength, uses maximum material for manufacturing and also takes highest time for manufacturing.

From this observation we can conclude that as we increase the infill percentage of the specimen it increases the total quantity of material used for manufacturing. Therefore it increases the weight of the specimen and for obvious reason it also increases the time required for the manufacturing.

4.3.2 Effect of Layer Height:

The following graphs gives an idea that changing layer height has some impact on tensile strength and manufacturing time but not much on the specimen weight.

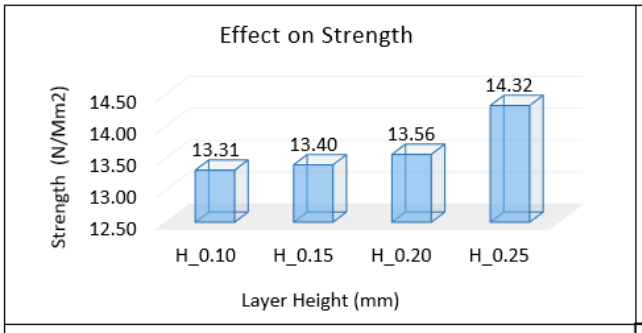

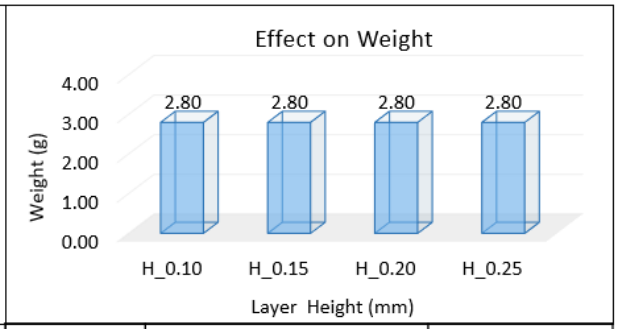

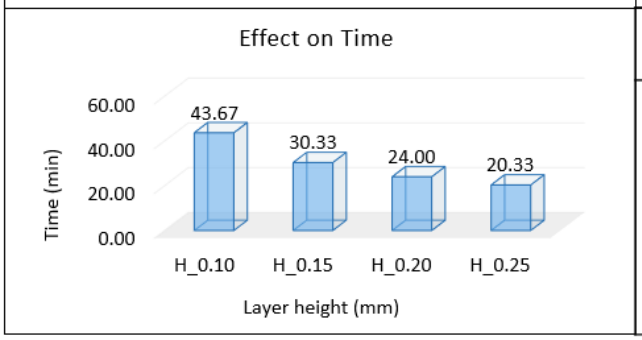

Parameter	Affecting Factor	Change
Increase in Layer Height	Strength of product	Increases
	Weight (Amount of Material required)	Constant
	Time for Manufacturing	Decreases

Figure 4-11 Effect of Layer Height on Tensile Strength, Product Weight and Manufacturing Time

From the graphical comparison it is clear that increase in layer height saves pretty good time for manufacturing as number of layers decreases with the increase in layer height. Decrement in number of layers saves time on number of iterations of layers. Therefore it saves pretty good time with increase in layer height. But after comparing strength graph it is ambiguous to conclude whether change in layer height affects the strength or not because there is very minor fluctuation in the tensile strength of the specimen after increasing the layer height. Still it shows consistent increase at minor level with the increase in layer height. We can develop hypothesis that as number of layers decreases number of bonds also decreases which decreases chances of delamination that is why it increases the strength.

At the same time, material graph shows pretty constant results even after increasing the layer thickness. The main reason behind such behavior is that even after increasing layer thickness the final dimensions of the specimen are similar. Therefore total volume of the required material stays constant even after making changes in layer height.

4.3.3 Effect of Number of Shells:

Number of shells decides the wall thickness of the specimen. Following graphs gives detail picture of variation in strength and material requirement with respect to the change in number of shells.

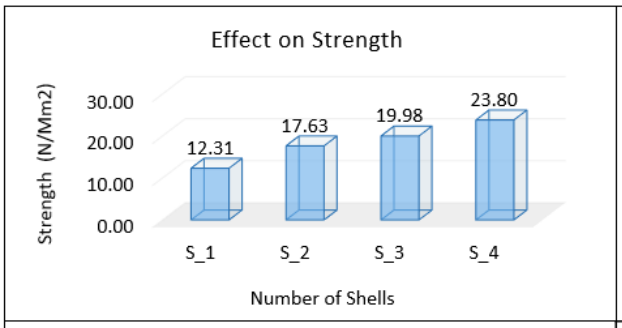

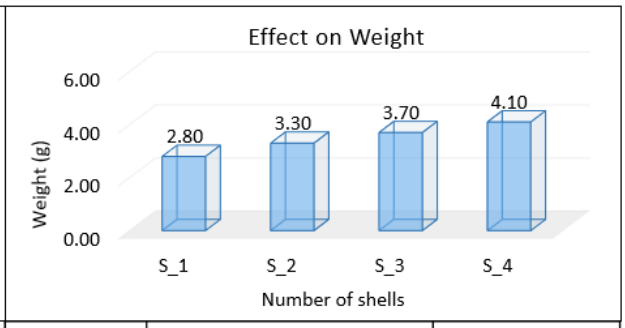

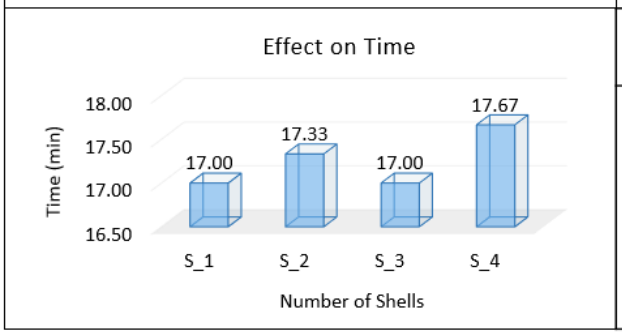

Parameter	Affecting Factor	Change
Increase in No of Shells	Strength of product	Increases
	Weight (Amount of Material required)	Increases
	Time for Manufacturing	Constant

Figure 4-12 Effect of Number of Shells on Tensile Strength, Product Weight and Time

Fig.14 shows that variation in number of shells make high impact on the strength of the specimen. As number of shells are increased, the specimen provides higher strength and the amount increase is pretty much consistent at each stage of change. It is observed from the graphs that increase in number of shells increases the number of iterations on the perimeter of the specimen which indirectly increases the weight of the material required for manufacturing.

But the graphical comparison of time with respect to number of shells shows some contradictory results. In all cases the time required for manufacturing is almost similar and it do not vary much as per

variations in number of shells. There are still chances that effect over time may vary with respect to changes in the geometry and size of the product.

4.3.4 Effect of Plane Orientation:

The following charts show the variation of tensile strength, weight and manufacturing time for different orientations of the plane.

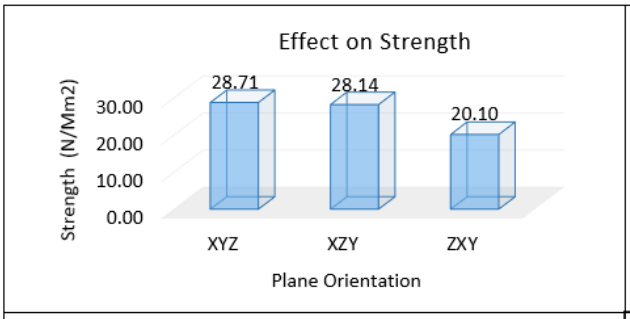

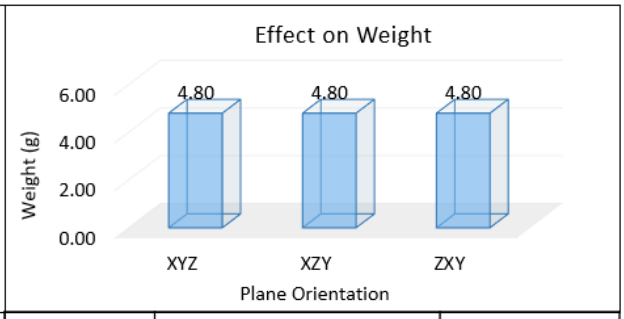

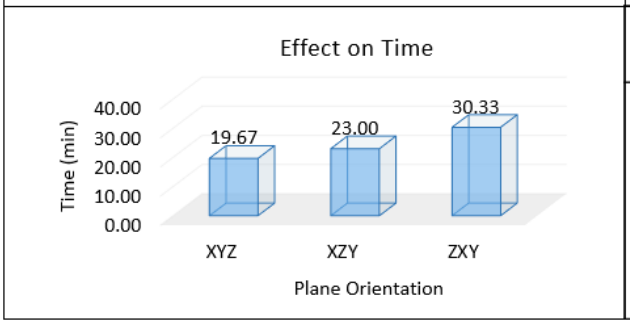

Parameter	Affecting Factor	Change
Plane Orientation	Strength of product	Best along Perpendicular direction
	Weight (Amount of Material required)	Constant
	Time for Manufacturing	Max in Z-direction

Figure 4-13 Effect of Plane Orientations on Tensile Strength, Product Weight and Time

In this case, XYZ and XZY plane shows pretty close results in aspect of strength. While specimen in ZXY plane show least strength as all layers are getting delaminated rather than going under fracture. Therefore it is considered as XYZ and XZY plane has the highest and similar strength while ZXY shows the least strength.

It is also visible that XYZ plane take least time for manufacturing while ZXY takes maximum time. The reason behind this is in XYZ plane orientation sample is built along the thickness of the specimen. In XZY plane orientation it is built along the width of the specimen and in case of ZXY plane it is built along the length of the specimen. Therefore in each case the number of layers varies because of the changes in the built length. XYZ plane had least built length so it was successfully done in minimum number of layers which saved most of the time for manufacturing. Similar way variation in time differs for other planes.

4.4 DISCUSSION:

In this study we discussed influence of different parameters on 3D printed structures. We completed experimental study to discuss the effect of Infill percentage, number of shells, layer height and plane orientation. Experimental study gives clear picture of the effect of all these parameters on strength, manufacturing time and material weight. But it is very important to understand the logics behind the study. There are also many other factors involved in 3D printing manufacturing which affects the final results. The most important factor is the geometry of the product. So with changes in geometry there are chances of getting some contradictory results to results discusses above.

It is clear that for all cases results for infill percentage will remain similar because as we increase the total infill percentage no matter what it is going to increase the material quantity and also it will take extra time for manufacturing. Therefore our results are very appropriate regarding the influence of infill percentage.

In case of layer height, it is pretty sure that if we increase the layer height it is going to reduce the time for manufacturing. And also the material quantity is not going to fluctuate because of any other factors. But few concerns are still involved when it comes up towards the tensile strength of the specimen. There if no confirm variation in the tensile strength of the material due to change in layer height. Also there are chances that for different combination of plane orientations layer height variation may affect differently. Even though we cannot confirm the exact variation of tensile strength with respect to changes in layer height, at least we were able to conclude from this study that there is very minor fluctuation in the tensile strength and approximately we can consider it to be constant.

Similar way variation of number of shells also depends on the geometry of the product. But in most of the cases it is going to improve the strength as it increases the outer wall of the product. On the other side it is very important to understand the behavior of 3D printed products under different plane orientations with most of the combination of raster orientations. Because every raster combination is going to make a difference in the effect of plane orientation. Therefore it is necessary to understand to combine effect of raster and plane orientation on the final strength of the product.

Chapter 5

FRACTURE TOUGHNESS OF 3D PRINTED STRUCTURES

5.1 INTRODUCTION

The major of stress required to inseminate the crack present in the structure is known as fracture toughness. Flaws could be because of cracks, air gaps, manufacturing errors or any other. As we cannot assure if the material is flaw free engineers have to take care of all scenarios considering the maximum flaw that could be available in the structure. So all critical designs are developed with the consideration of different flaws in the structures. This kind of approach benefits to develop study with respect to different error dimensions, geometry of the structure, loading conditions and material property which is known as Fracture Toughness.

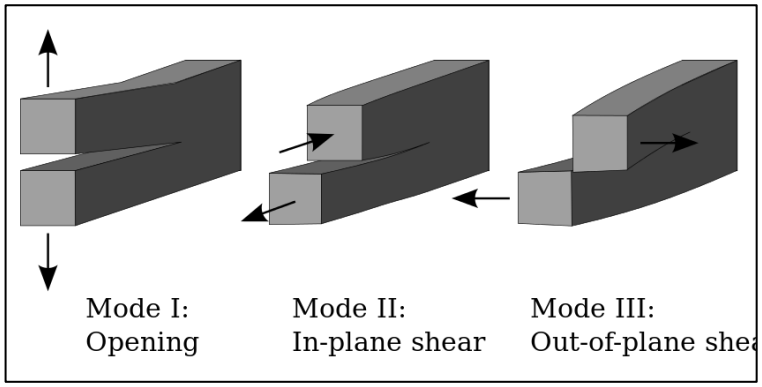

Figure 5-1 Modes of Fracture Failures [13]

As additive manufacturing is getting popular in most of the fields especially in medical, automotive and aerospace engineering it is highly important to study the behavior of crack propagation of 3D printed structures. The presence of crack in the structure can convert the local stresses to failure stresses no matter how carefully it is designed by engineers. Sometimes even though the stresses are far less than the failure limit in different loading conditions, the material may fracture because of the presence of the crack in the structure as crack propagates easily because of the load. Therefore in this research study we tried to experimentally investigate whether current fracture mechanics relations are applicable for samples fabricated using additive manufacturing or not. It is thought-provoking to analyze how a single design manufactured by different processing parameters gets affected under a crack growth.

5.2 ANALYTICAL STUDY

In this study we focused on mode I type of fracture mechanics. That considers the infinite plate for uniform uniaxial stress. Idea of this study is to validate the traditional fracture mechanics theory for 3D printed specimens and calculate the stress intensity factor of each specimen fabricated under different parametric conditions.

The stress intensity factor, K, is a parameter that amplifies the magnitude of the applied stress. Stress intensity in any mode situation is directly proportional to the applied load on the material. If a very sharp crack can be made in a material, the minimum value of KI can be empirically determined, which is the critical value of stress intensity required to propagate the crack [14] .This critical value determined for mode I loading in plane strain is referred to as the critical fracture toughness KI of the material.

Stress Intensity Factor can be calculated as,

$$K_I = \sigma_t . \sqrt{\pi . a}$$

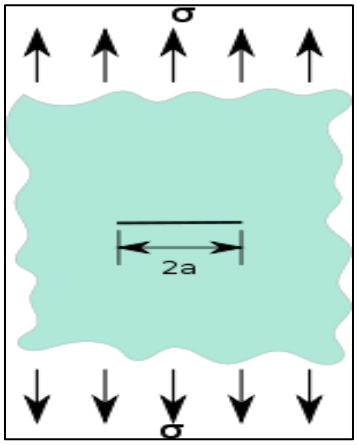

Figure 5-2 Mode I Fracture [15]

The Mode I critical stress intensity factor, KI is the most often used engineering design parameter in fracture mechanics and hence must be understood if we are to design fracture tolerant materials used in bridges, buildings or aircraft.

5.3 EXPERIMENTAL STUDY

5.3.1 Specimen Design and Construction:

For the study of crack propagation, flat plate shaped solid specimens were fabricated on MakerBot Replicator 2X using acrylonitrile butadiene styrene (ABS). Used 1.75mm diameter material filaments for the fabrication of specimens. General material properties of the ABS are specified in Table 3. The specimens were designed with an inbuilt central crack to study Mode I type of fracture under tensile loading as shown in Figure 5.3.

Table 3-1 ABS Material Properties [16]

Density	1.03 g/cm^3
Tensile Modulus	1.69 to 2.82 GPa
Poisson's Ratio	0.35
Glass Transition Temperature	104.44
Melting Temperature	No specific melting point

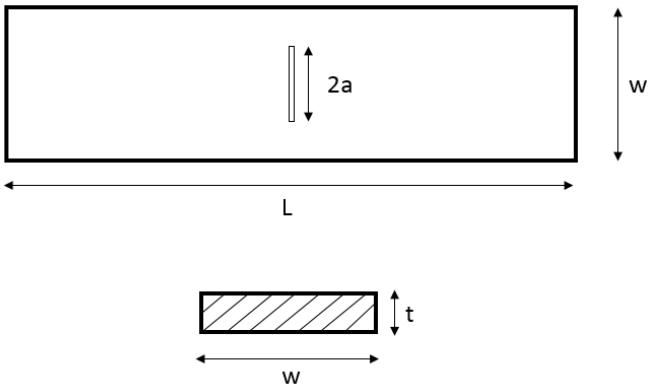

Figure 5-3 Specimen Design

Specimens were built using different process parameters as mentioned earlier. For applying variation to the parameters first fixed the defaults settings for the fabrication in such a way that Raster Orientation was set to 90°, Infill Percentage as 100%, Layer Height was set to 0.20mm, Number of Shells as 2 and built along the X-axis with the flat pattern. Then each parameter was focused separately holding other

parameters to default settings. In this manner, fabricated three specimens of each of the following parameter configurations,

I. Four different raster orientations : 0°, 30°, 60°, 90°

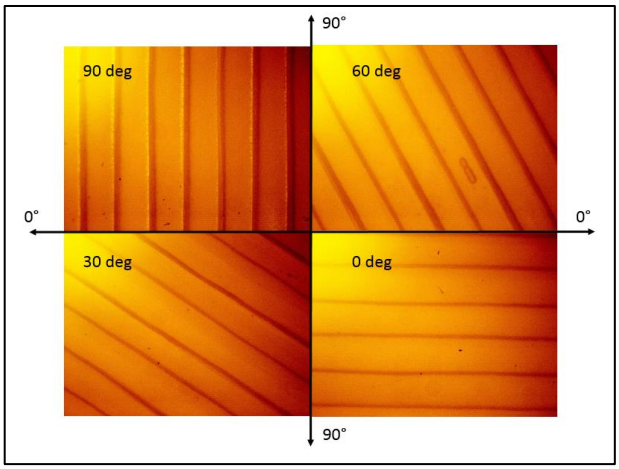

Figure 5-4 Microscopic View of Fiber Orientations

II. Total six different axis of orientations including three axis with two patterns of each: X-axis_Flat, X-axis_Verical, Y-axis_Flat, Y-axis_Vertical, Z-axis along X and Z axis along Y.

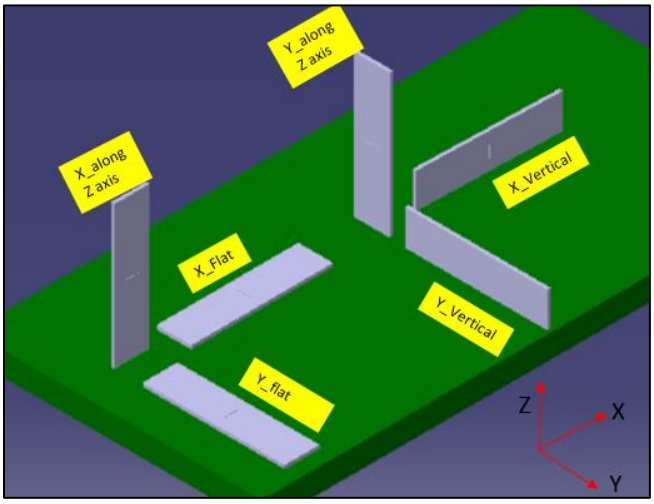

Figure 5-5 Samples in different Axis orientations

III. Three different infill percentage: 50%, 75%, 100%.

IV. Three different Layer Heights: 0.15mm, 0.20mm, 0.25mm.

V. Three different number of shells: 1 shell, 2 shells, 3 shells.

Other all settings of printer were set to defaults as mentioned in the Table 3-2,

Table 3-2 Printer Default Settings

SETTINGS	VALUE	SETTINGS	VALUE
EXTRUDER TEMPERATURE	230° C	Outline Print Speed	40 mm/s
PLATFORM TEMPERATURE	110° C	Infill Pattern	Linear
TRAVEL SPEED	150 mm/s	Roof Thickness	1.00 mm
FIRST LAYER PRINT SPEED	30 mm/s	Floor Thickness	1.00 mm
INFILL PRINT SPEED	90 mm/s	Coarseness	0.00010 mm

5.3.2 Specimen Testing:

All tensile testing were done using Shimadzu Autograph model AGS-X universal testing machine at room temperature conditions. Applied tensile force at the rate of 5 N/Sec till the fracture takes place. Fig.5.6 gives clear picture of the tensile machine fixture and the settings. Specimen was aligned perfectly vertical to avoid all twisting and shear forces.

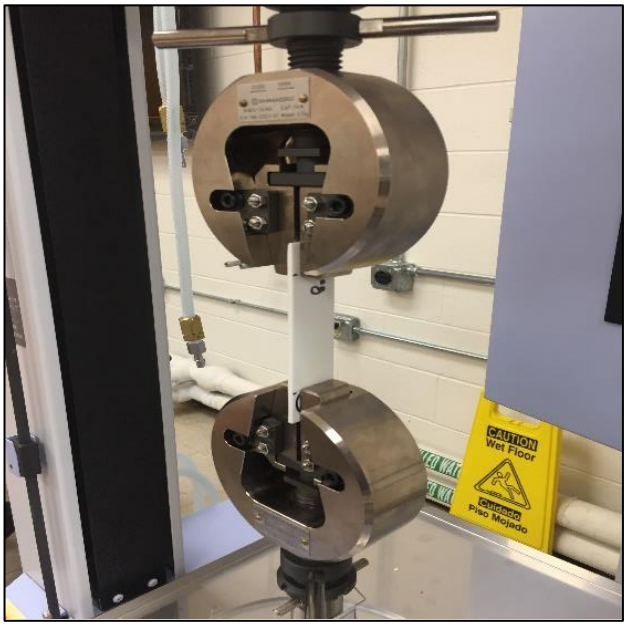

Figure 5-6 Tensile Testing

5.4 RESULTS AND ANALYSIS

All tests were completed to measure the tensile strength and stress intensity factor of each specimen fabricated under different parametric conditions. In the following part we will separately discuss the variation in tensile strengths of specimens under each parametric condition.

5.4.1 Raster Orientation:

Tensile tests results of raster orientation parameter are presented in Table. Results displays the variation in tensile strengths of specimen ranging from 0° to 90°. In this range noticeable increase of tensile strength can be observed in Figure 5.7. It is clearly detected that 0° specimen has the highest tensile strength while 90° specimens shows the least strength.

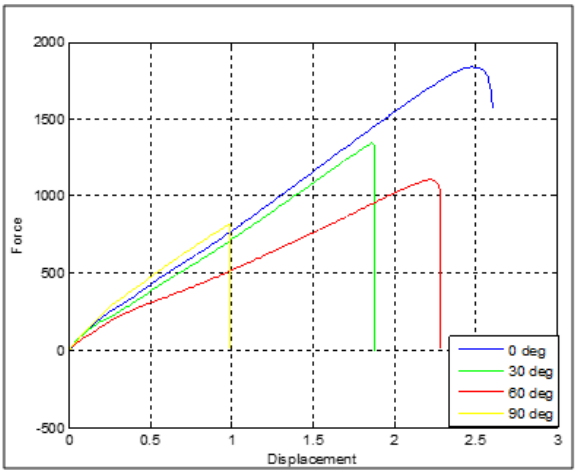

Raster Orientation	Mean Tensile Strength (N/mm2)	Stress Intensity Factor (K_I)
0 deg	20.69	81.95
30 deg	14.78	58.54
60 deg	12.46	49.34
90 deg	9.59	37.98

Figure 5-7 Tensile Test Data Analysis for Rater Orientation

Experimental study shows leading results for the 0° specimen in Figure 12. But it is very important to understand why there is consistent decrement in tensile strength from 0° to 90° specimen and why 0° specimen provides maximum tensile strength. It is observed that fiber orientation plays vital role in here. The specimen with 0° raster orientation has the maximum number of polymer molecules aligned along the force direction while the specimen with 90° orientation has maximum number of polymer molecules lateral to the force direction.

Fig. 5.8 displays clear picture of the effect of polymer alignment on the tensile strength. For 0° specimen, as all fibers are aligned along the direction of force, it tends to elongate along the force direction. Polymer molecules have a tendency to resist force at the maximum level under elongation. This way as more is the elongation more will be the resistance to the applied force. Therefore 0° specimen provides highest level of resistance to the applied stress. On the other side 90° raster orientated specimen have all the fibers aligned in a lateral direction to the applied force. This cause all fibers to bend under tensile stress condition. Under bending mode, polymers resist least to the tensile force. Therefore in this case fibers break very easily as compared to the 0° fiber alignment. That way as fibers get orientated from 0° to 90°, the tendency of elongation of polymer molecules decreases and hence the tensile strength.

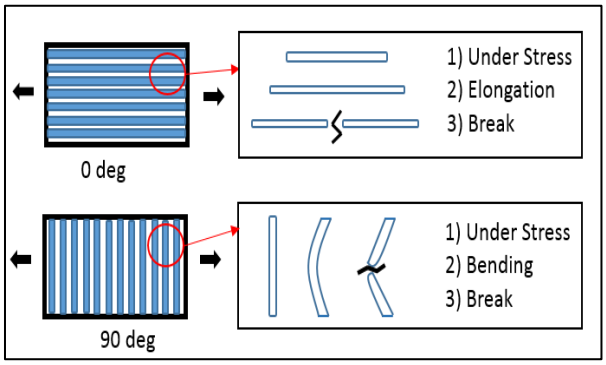

Figure 5-8 Polymer behavior under tensile stress

5.4.2 Axis Orientation:

Summary of the mean tensile strength and stress intensity factor is presented in Table 3. The variation in axis orientation shows visible effect on the strength of the specimen. Graphical variation in the tensile strengths of the specimens is presented in Figure 5.9.

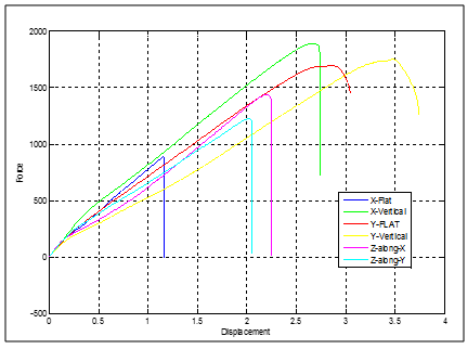

Axis Orientation	Mean Tensile Strength (N/mm2)	Stress Intensity Factor (K_I)
X-Axis_Flat	9.05	35.83
Y-Axis_Flat	19.08	75.59
Z-Axis _along X	15.01	59.43
X-Axis_Vertical	21.57	85.45
Y-Axis_Vertical	19.72	78.11
Z-Axis _along Y	12.57	49.80

Figure 5-9 Tensile Test Data Analysis for Axis Orientation

Considering theory discussed earlier in raster orientation section, it was supposed to get higher tensile strength along the Y-axis pattern as all the fibers are aligned along the force direction. But in this case results contradicts to the previous discussion. Data results indicates that X-Axis-Vertical has better strength than the specimens built along the Y-Axis-Vertical and Y-Axis-Flat direction. Therefore this results forces to further study the behavior of polymer fibers bonded together.

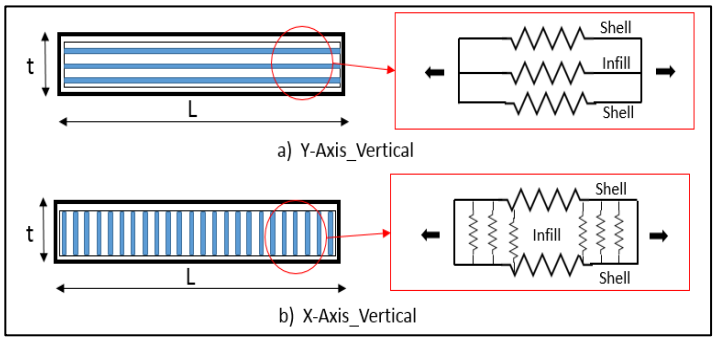

Figure 5-10 Spring Behavior of Polymer Fiber

Detail observation on the polymer behavior is considered as shown in Figure 23. For the case of X-Axis-Vertical specimen, it is assumed that because of higher length to thickness ratio infill fibers tends to provide higher resistance against bending. Under tensile loading condition infill fiber polymers starts bending along the applied force. But due to shorter length along the thickness fiber do not break immediately after bending. Instead it provides spring action kind of behavior. This way outer shells that are under elongation get supported by the infill fibers aligned in a lateral direction of the applied force. Therefore X-Axis-Vertical specimen get higher resistance towards tensile loading due to shorter size of the thickness and hence provides highest tensile strength.

On the other side, Y-Axis_Vertical specimen has all the fibers oriented along the direction of the force. Therefore all of the fibers undergoes elongation once tensile stress is applied. That means this sample exhibits exact behavior as mentioned in the case of 0° specimen. Overall it is conceivable that fibers shows the high strength when aligned along the direction of the force but it provides better strength under some particular conditions as discussed.

5.4.3 Layer Height:

Tensile test results for layer height variation are presented here. Figure 5.11 presents variation in tensile strengths with the change in layer heights. Results displays inferior decrease of tensile strength as we increase the layer height of the specimen. Table below displays comparison of each iteration done for the different layer heights and it shows there is very minor difference between the tensile strengths.

It is observed that lesser layer height tends to increase the number of layers for the fabrication. As number of layer increases, it also increases the number of bonds between the top and bottom part of the specimen. Therefore when specimen is affected by a tensile loading the stress get distributed in more number of locations resulting in bit higher resistance towards tensile force. That way lesser layer height provides little bit higher tensile strength.

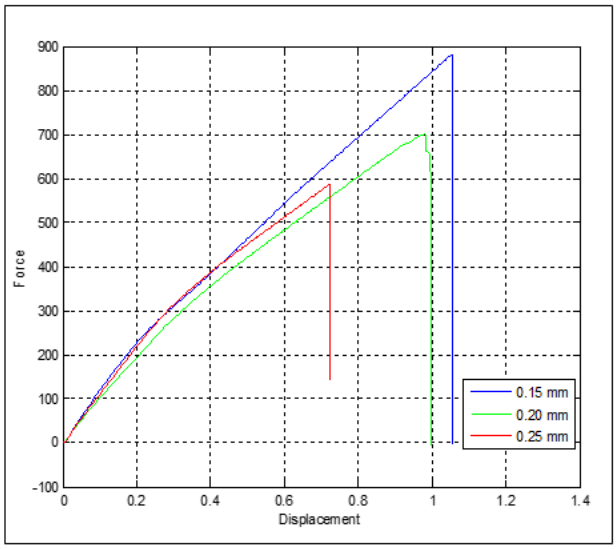

Layer Height	Mean Tensile Strength (N/mm2)	Stress Intensity Factor (K_I)
0.15 mm	9.19	36.40
0.20 mm	8.27	32.76
0.25 mm	7.60	30.11

Figure 5-11 Tensile Test Data Analysis for Layer Height

Even though layer height does not affect much to the tensile strength still it is very important parameter to be considered for the manufacturing. It is identified that smaller layer height consumes more time and at the same time provides higher finishing to the prints. Thus smaller layer height deliver higher quality, tensile strength and consumes more time.

5.4.4 Infill Percentage:

Figure 5.12 shows graphical representation of tensile tests for variation of infill percentage in 3D printed specimen. Summary of the mean tensile strength and stress intensity factor is presented in Table. The variation in infill percentage shows visible effect on the tensile strength of the specimen.

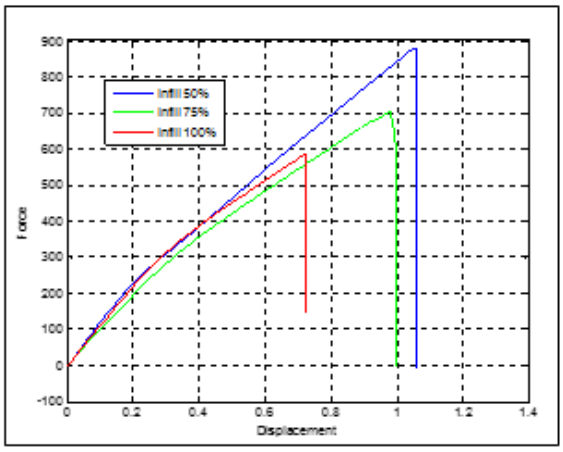

Infill Percentage	Mean Tensile Strength (N/mm2)	Stress Intensity Factor (K_I)
50%	7.47	29.61
75%	9.16	36.30
100%	11.02	43.66

Figure 5-12 Tensile Test Data Analysis for Infill Percentage

5.4.5 Number of Shells:

Fig.5.13 shows graphical representation of tensile tests for variation of number of shells in 3D printed specimen. Summary of the mean tensile strength and stress intensity factor is presented in Table. The variation in number of shells shows visible effect on the tensile strength of the specimen.

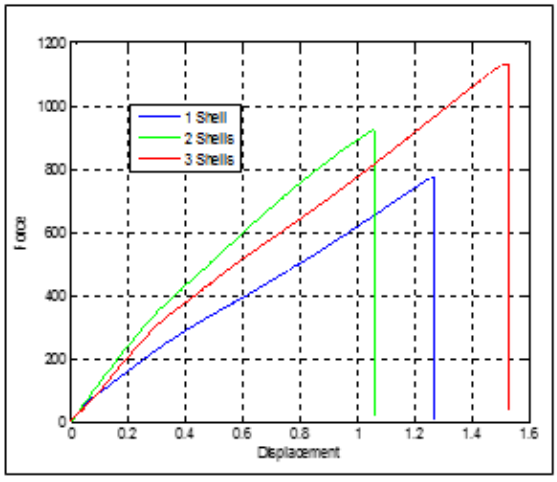

Number of Shells	Mean Tensile Strength (N/mm2)	Stress Intensity Factor (K_I)
1 Shell	8.30	32.89
2 Shells	10.04	39.75
3 Shells	11.72	46.43

Figure 5-13 Tensile Test Data Analysis for Number of Shells

5.4 DISCUSSION

Complete review of the fractured specimen draws attention to the fact that there is a noticeable variation in the path of the crack propagation depending upon the direction of fiber orientations. Figure 5.14 gives more clear view of the fractures that took place under different raster orientations. It is observed that the presence of crack in the structure initiates the fracture and it propagates along the inter fiber bonding of the specimen. In FDM manufacturing method, the inter fiber bonding is the weakest zone in the structure due to various reasons. That is the major factor affecting the strength of the specimen and at the same time affects the fracture. When external forces are applied, residual stresses strike the weakest zone and follows the path resulting in the crack propagation. Exactly the same behavior can be observed particularly in the case of 30°, 60° and 90° fiber oriented specimen.

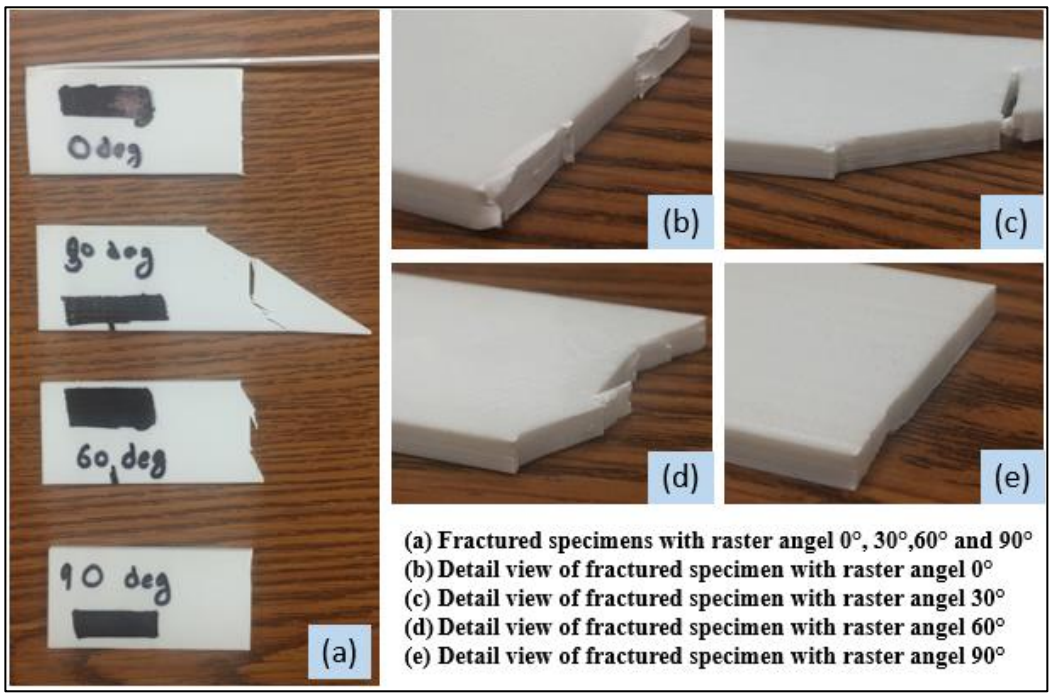

Figure 5-14 Fractured Specimens with Different Raster Orientations

In the case of 0° specimen all the fibers were aligned along the direction of the force which showed some arbitrary fracture behavior. In this case, when force is applied, structure started breaking fibers close to the crack and instead of propagating along the inter fiber bonding it started breaking fibers one by one

along the direction of the crack. Then specimen was lengthen until last outside fiber supports the structure. This kind of behavior justifies the result of getting higher strength in 0° specimen.

There is a clearly visible white colored zone appearing during the deformation of the specimens due to crazing of the polymer. Figure 5.14 part (b) highlights one of the clear picture of this white zone in specimen with 0° raster orientation. Crazing is a significant mechanism by which the polymer absorbs energy which prevents fracture [9]. The craze band formation is observed in the lateral direction to the tensile loading. And it is also observed that the craze formation zones displays highest level of deformations resulting in higher strength.

Microscopic study of the specimen gives better understanding of the reasons behind the variation in the strengths and mode of fractures of different specimens. It is observed that bonding between neighboring fibers and air gaps between them has a huge impact on the final strength of the structure.

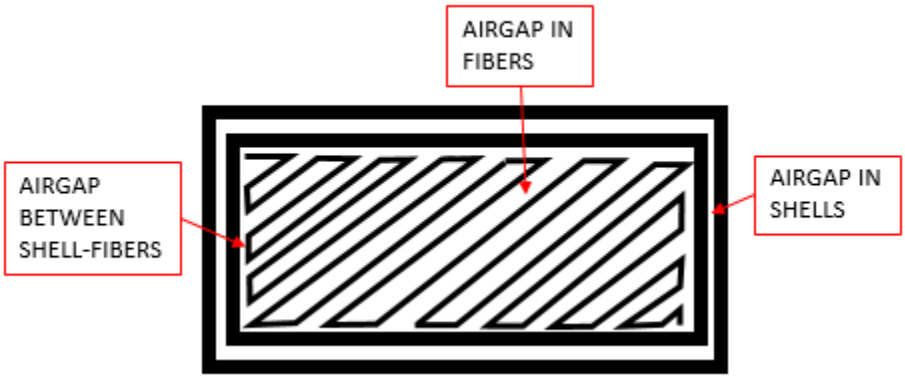

Figure 5-15 Exaggerated Schematic Showing Airgaps on Each Layer of Specimen

Additive manufacturing is a kind of free form of manufacturing technique where no external loadings are applied while manufacturing the structure. This is one of the main reason of having a space for airgaps in the 3D printed specimen. Figure 19 illustrates the magnified view of 3D printed layer consisting of air gaps of different locations. These airgaps in the layers and shells weaken the bonding between them which basically affects the strength of the structure. Our study also suggests that chances of getting more cracks are very high due to airgaps.

5.5 SUMMARY AND CONCLUSION

From this study it is understood that processing parameters make a very much impact on the fracture toughness of the additive manufactured ABS structure. The specimen with raster orientation of 0° has highest fracture strength and it decreases with the increase in angle of raster orientation considering loading is along 0°. Axis orientations also makes impact along with the raster orientations. For the case of 0° raster oriented specimen, X-Axis-Vertical shows the highest fracture strength following with Y-Axis-Vertical pattern. The X-Axis-Flat pattern provides least strength in this case. It is very important to understand from this study the variation in axis and raster orientation makes difference in final strength because of the polymer fiber alignment with respect to the direction of applied force. Therefore basic study on external force application and fiber alignment will help to predict the best configuration for highest strength in the structure.

It is found that layer height does not affect much to the tensile strength still it is very important parameter to be considered for manufacturing. It is identified that smaller layer height consumes more time and at the same time provides higher finishing to the prints. Thus smaller layer height deliver higher quality, tensile strength and consumes more time. Adding to that infill percentage and number of shells also makes large impact on the fracture toughness as it provides stronger and stiffer structure in some way. Increase in these two parameters provide higher strength to the structure.

It is observed that other than these parameters, strength is also affected by some parameters like air gaps and width of the extruded fiber. These are major factors which could not be controlled for now. Therefore more studies are required to make additive manufacturing more effective.

CHAPTER 6

EFFECT OF RASTER ORIENTATION ON 3D PRINTED STRUCTURES

6.1 INTRODUCTION

Previous chapters talk about the dependence of FDM mechanical properties on the various directions and processing parameters involved in manufacturing. And it is very important to verify this effect on different materials. The idea of this work is to understand the behavior of FDM parts manufactured by ULTEM -9085 along different raster orientations and planes. It is very important to clarify whether built material maintains the strength along different orientations under different loading conditions. Therefore in this work tensile and shear strength properties of 3D printed specimens are tested and analyzed to conclude its behavior.

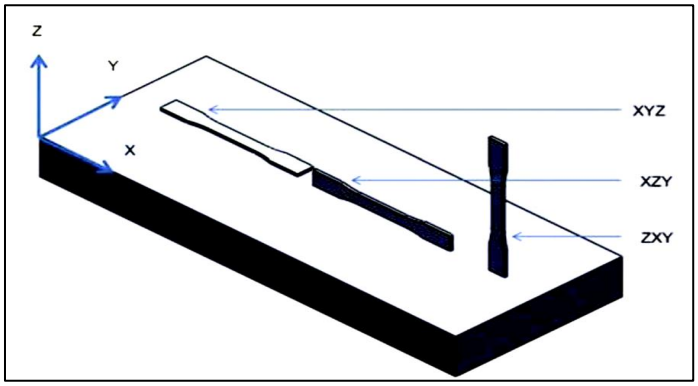

Figure 6-1 Different Plane Orientations

6.2 EXPERIMENTAL APPROACH AND METHODS

6.2.1 Material:

All of the FDM specimens tested and analyzed in this study were ULTEM-9085 resin. ULTEM™ 9085 resin is a flame-retardant high-performance thermoplastic for digital manufacturing and rapid prototyping. It is ideal for the transportation industry due to its high strength-to-weight ratio and its FST (flame, smoke and toxicity) rating. This unique material's preexisting certifications make it an excellent choice for the commercial transportation industry – especially aerospace, marine and ground vehicles.

Combined with a Fortus® 3D Production System, ULTEM 9085 allows design and manufacturing engineers to produce fully functional parts that are ideal for advanced functional prototypes or end use without the cost or lead time of traditional tooling.

6.2.2 Specimen Construction:

This project included three different mechanical tests: tension, short beam shear and Iosipescu test. For each test three unique specimen designs were designed and manufactured. The tension specimens were all thin rectangular slabs fabricated to be 115 mm long, 19 mm wide, and 3 mm thick in accordance with ASTM D638.

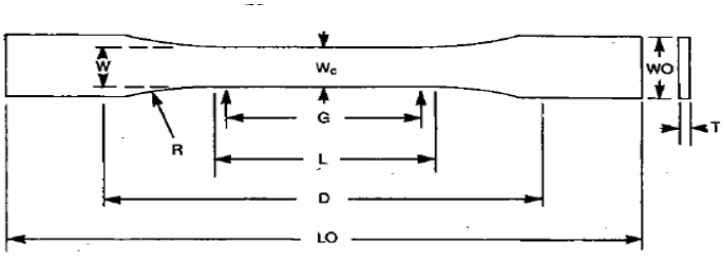

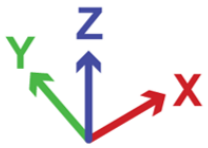

Specimen Dimensions for Thickness, *T*, mm (in.)[A]

Dimensions (see drawings)	7 (0.28) or under	
	Type I	Type II
W—Width of narrow section[E,F]	13 (0.50)	6 (0.25)
L—Length of narrow section	57 (2.25)	57 (2.25)
WO—Width overall, min[G]	19 (0.75)	19 (0.75)
WO—Width overall, min[G]	...	...
LO—Length overall, min[H]	165 (6.5)	183 (7.2)
G—Gage length[I]	50 (2.00)	50 (2.00)
G—Gage length[I]	...	...
D—Distance between grips	115 (4.5)	135 (5.3)
R—Radius of fillet	76 (3.00)	76 (3.00)
RO—Outer radius (Type IV)	...	...

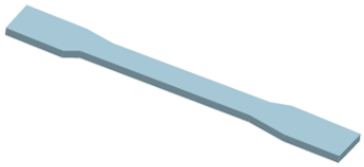

Figure 6-2 Specimen construction as per ASTM D638 for Tensile Test [17]

For short beam shear test the geometry was rectangular block of 27 mm long, 9 mm wide and 4.5 mm thick in accordance with ASTM D2344.

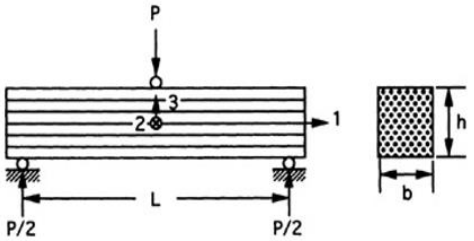

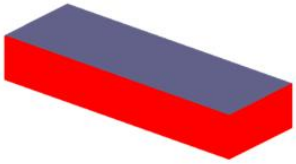

Figure 6-3 Specimen construction as per ASTM D2344 for Short Beam Shear Test

For the Iosipescu test, the V-notch specimen was modeled within the computer solid model of the specimen and was produced directly on the FDM machine as per ASTM D5379.

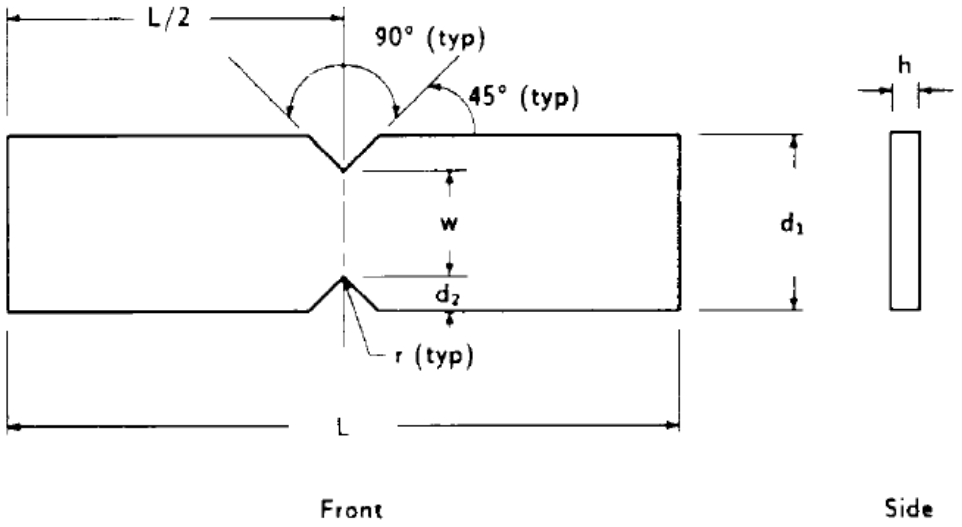

Nominal Specimen Dimensions

d_1	=	20.0 mm [0.75 in.]
d_2	=	4.0 mm [0.15 in.]
h	=	as required
L	=	76.0 mm [3.0 in.]
r	=	1.3 mm [0.05 in.]
w	=	12.0 mm [0.45 in.]

Figure 6-4 Specimen construction as per ASTM D5379 for Iosipescu Test [18]

For all tests specimens were built along three different planes, XYZ, XZY and ZXY. In each plane specimens were manufactured with different raster orientations. For tensile test raster orientations used were 0°, 15°, 30°, 45° and 90° Unidirectional specimens and also some combinations of alternating layers such as 15°/ 105° , +45° / -45° and 0° / 90° were manufactured. For tensile test raster orientations used were 0° Unidirectional and alternate combination of +45° /-45° and 0° / 90° were manufactured. For Iosipescu test raster orientations used were 0°, 90° Unidirectional and alternate combination of +45° /-45° were manufactured.

Table 6-1 Total Count of all Specimens Manufactured

	TENSILE TEST			SHORT BEAM SHEAR			IOSIPESCU TEST			
Planes Orientation	**XYZ**	**XZY**	**ZXY**	**XYZ**	**XZY**	**ZXY**	**XYZ**	**XZY**	**ZXY**	**TOTAL**
0 °_UD	10	10	5	5	3	3	5	3	3	**47**
15 °_UD	6	6	3							**15**
30 °_UD	6	6	3							**15**
45 °_UD	10	10	5							**25**
90 °_UD	10	10	5				5	3	3	**36**
15° / 105 °	6	6	3							**15**
+45° / -45 °	10	10	5	5	3	3	5	3	3	**47**
0° / 90°	10	10	5	5	3	3				**36**
TOTAL	**68**	**68**	**34**	**15**	**9**	**9**	**15**	**9**	**9**	**236**

6.2.3 Mechanical Testing:

Tension tests were first completed, per the ASTM D638 standard, in order to determine the mean ultimate tensile stress (UTS) and effective modulus of elasticity along the longitudinal loading direction for each of the different raster orientations. Different number of specimens of each of orientations (Total 170) were tested on a Shimadzu AGS-X universal testing machine with ±0.5% accuracy and 5kN load capacity. Tests were run with grip speed of 5 mm/min. Each tension specimen was pulled until fracture occurred.

As shown in Fig. all specimens were affixed with Epsilon extensometer of 25mm gauge length to record transverse displacements during tension testing, from which tensile strains were estimated. Short beam shear tests and Iosipescu tests were performed according to ASTM D2344 and ASTM D5379, in order to determine the shear stress and approximate shear modulus for different raster orientations. Different number of specimens of each of orientations (Total 33) were tested on a Shimadzu AGS-X universal testing machine with ±0.5% accuracy and 5kN load capacity. Tests were run with grip speed of 2 mm/min for short beam shear test and 1.2 mm/min for Iosipescu test. Setup of both testing methods are shown in following pictures,

Figure 6-5 Experimental setup for Tensile, Short beam shear and Iosipescu test

6.3 ANALYTICAL STUDY:

6.3.1 Tensile Test:

Calculated the tensile strength by dividing the maximum load in Newton (or pounds-force) by the original minimum cross-sectional area of the specimen in square Meters.

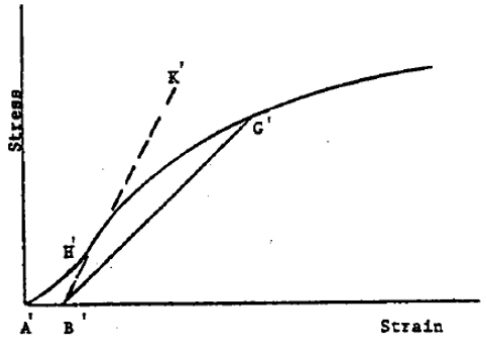

Stress = P / A
where,
P → Force (N)
A → Cross section area (mm^2)

Strain = D / L
where,
D → Displacement
L → Length

6.3.2 *Short Beam Shear test:*

It is not possible to obtain shear strain data without using strain gauge and use of strain gauge is unreliable because of non-smooth surface finish. Therefore we followed formulation as shown below,

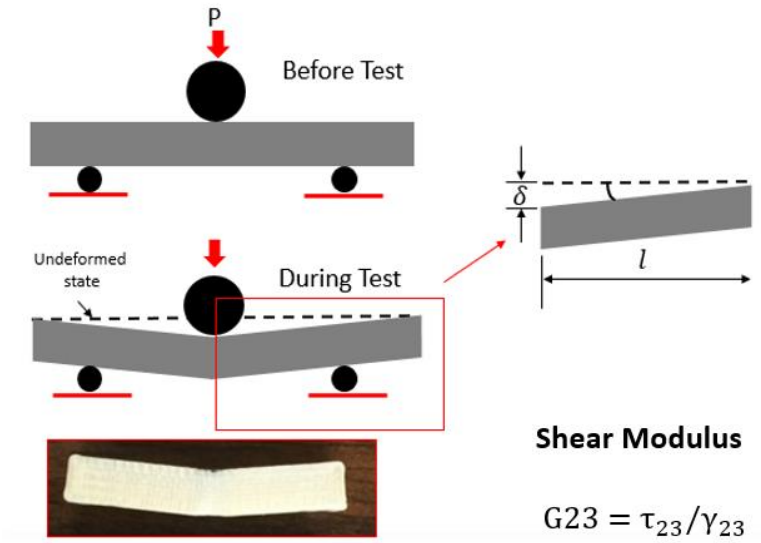

Shear Stress (ASTM D2344)

$$\tau_{23} = 0.75\frac{P}{bh}$$

Shear Strain(approximate)

$$\gamma_{23} = tan^{-1}\left(\frac{\delta}{l}\right)$$

δ = Machine cross-head reading
l = half span of the short beam specimen

Shear Modulus

$$G23 = \tau_{23}/\gamma_{23}$$

6.3.3 *Iosipescu Test:*

Similar to short beam shear test, it is not possible to obtain shear strain data without using strain gauge and use of strain gauge is unreliable because of non-smooth surface finish. Therefore we followed formulation as shown below,

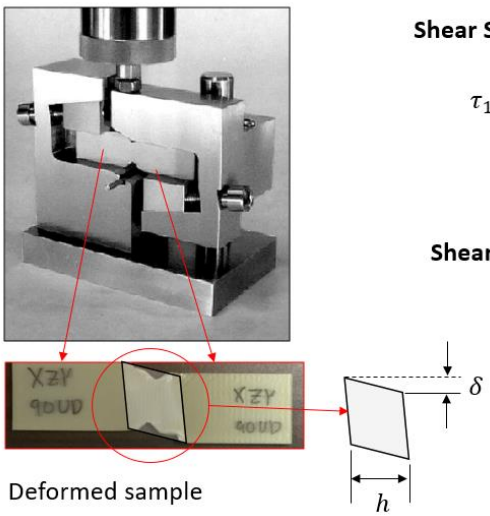

Shear Stress (ASTM D5379)

$$\tau_{12} = \frac{P}{A}$$

Shear Strain (approximate)

$$\gamma_{12} = tan^{-1}\left(\frac{\delta}{h}\right)$$

where,
δ = Machine cross-head reading
h = vertical distance between shear deformed zone

Shear Modulus,

$$G_{12} = \frac{\tau_{12}}{\gamma_{12}}$$

6.4 RESULTS AND DISCUSSION:

6.4.1 Tensile Test Results :

1) XYZ Plane:

Summary of the tension test results for different raster orientations in XYZ plane are graphically shown in Fig. 6.6. The mean ultimate strengths was largest for the longitudinal 0° raster orientation, 69.58 MPa and weakest for the transverse 90° raster orientation, 19.48 MPa. There is very systematic pattern of decrement in tensile strengths along the increase of raster orientations from 0° to 90°. But it can be seen that specimens with alternating lamina shows very close results to each other which is in the range of 52 to 28 MPa.

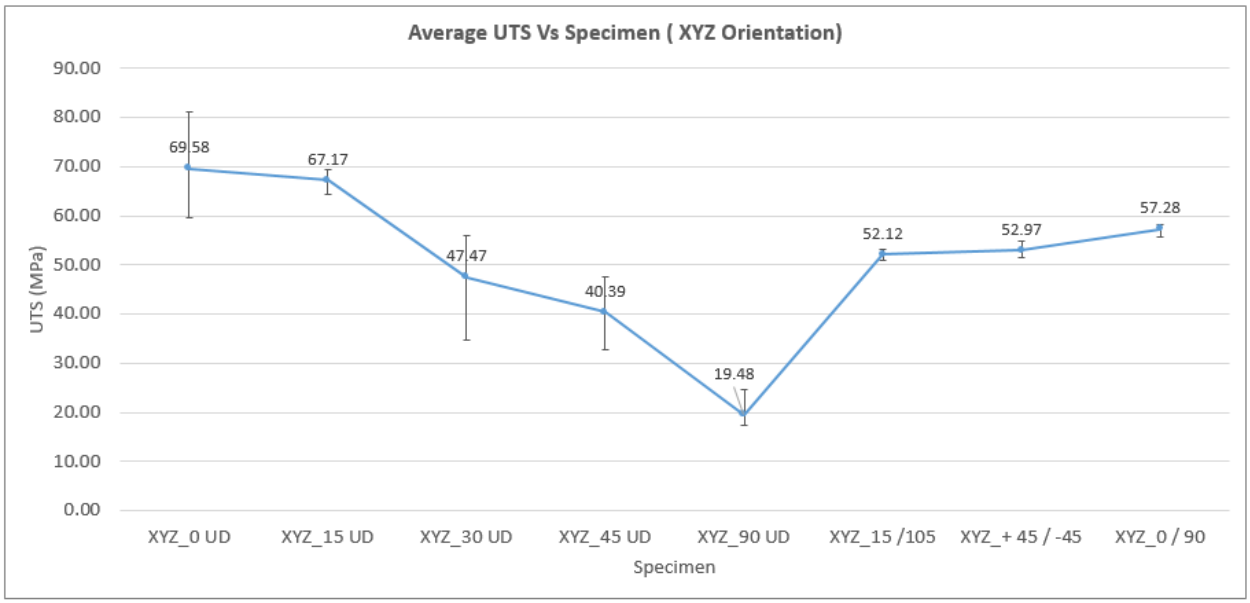

Figure 6-6 Comparison of ultimate tensile strength for different raster orientations along XYZ plane

Even though Fig. 34 shows average ultimate strength along 0° specimen was largest, detail evaluation of each specimen shows some contradictory results. Fig 35 shows that three specimens with 0° raster orientation has less ultimate strength than 15° raster oriented specimens which is irregular behavior for 3D printed structures. Therefore it is necessary to investigate the root cause for this irregular behavior. Hence we checked data for each iterations and compared each result graphically as shown in Fig 6-7

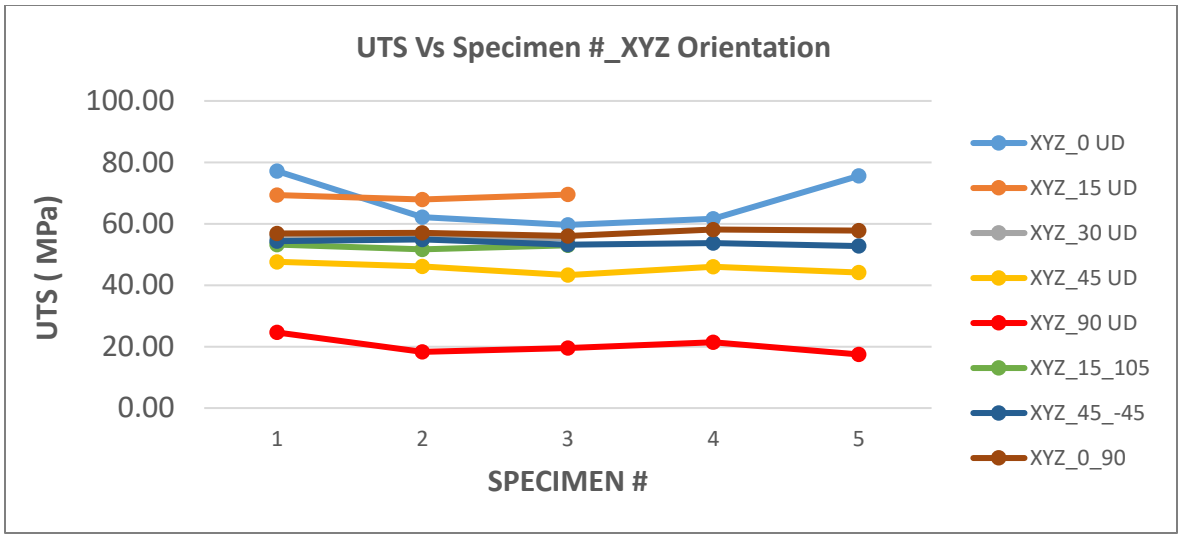

Figure 6-7 Graphical comparison of ultimate tensile strength for each specimen of different raster orientation along XYZ plane

After investigating each and every broken specimen, it is clear that specimen showing irregular strength had some voids at the curve part of the specimen which resulted in stress concentration at the curved area. That is why most of the specimen broke at the grip and not on the middle cross section of dog-bone. It was too complicated to measure the cross section area along the contour as shown in figure below. Therefore we could not get an appropriate values for ultimate strength. Hence we discarded results of XYZ_0° UD dog-bone specimen.

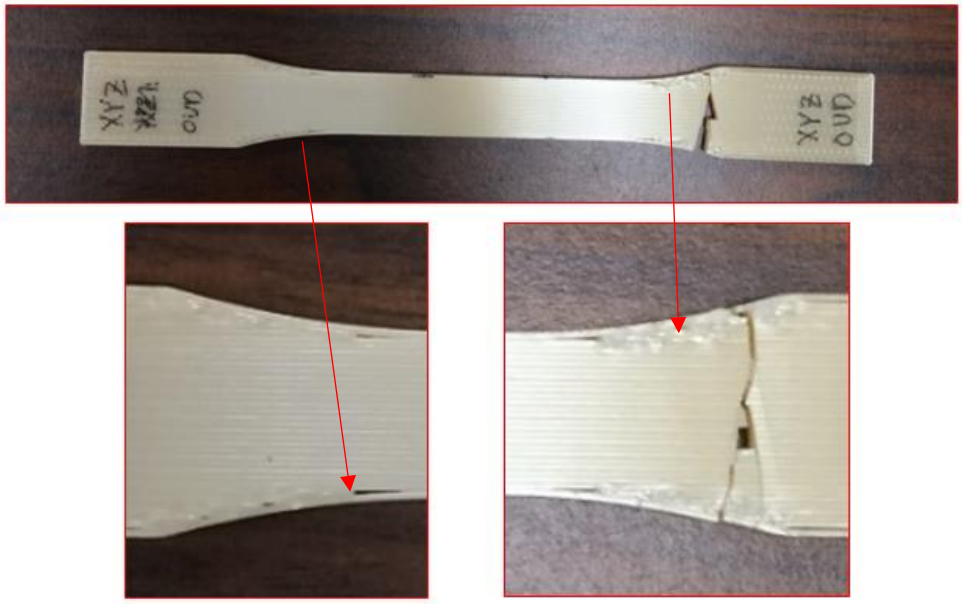

Figure 6-8 Investigation of XYZ_0° UD dog-bone specimen

2) Straight Bar Coupons:

XYZ_0° unidirectional dog-bone specimen were discarded because of irregular behavior along the contour. Therefore to study the behavior of 3D printed structure along the 0° unidirectional loading conditions, we replaced straight bar coupons with dog bone specimen. And the results of straight bar coupons with different combinations of raster orientations are as shown below,

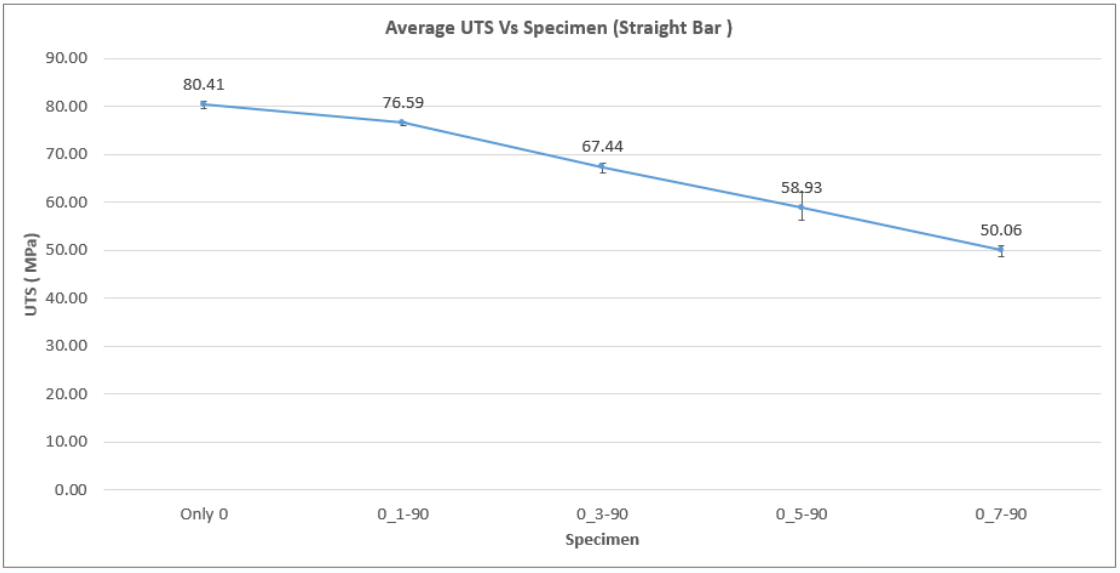

Figure 6-9 Graphical comparison of ultimate tensile strength of straight bar coupons along XYZ plane

Figure 6.9 shows maximum ultimate strength of 80.41 MPa when specimen is manufactured with only 0° layers. But as we increase the number of layers of 90° raster orientation, the ultimate strength decreases consistently. Therefore the specimen with 7 layers of 90° orientation shows the least ultimate strength of 50.06 MPa. In this case we found two different types of failures, one is in midway of the specimen and the other failure was near to the grip. Figure 6.10 gives clear picture of failure types.

Figure 6-10 Failure types of straight bar coupons

3) XZY Plane:

Summary of the tension test results for different raster orientations in XZY plane are graphically shown in Fig. 6.11. The mean ultimate strengths was largest for the longitudinal 0° raster orientation, 83.27 MPa and weakest for the alternate layered 15° / 105° raster orientation, 63.62 MPa. In this case the range of variation in ultimate strength is very less as compared to the XYZ plane. But there is irregular behavior observed in the case of 15° unidirectional raster orientation specimen. As per regular behavior of 3D printed structures 15° unidirectional specimen should provide higher strength than 30° and 45° raster oriented specimen but it is contradicting in this case. Therefore each specimen was investigated to find the main reason of this anomalous behavior.

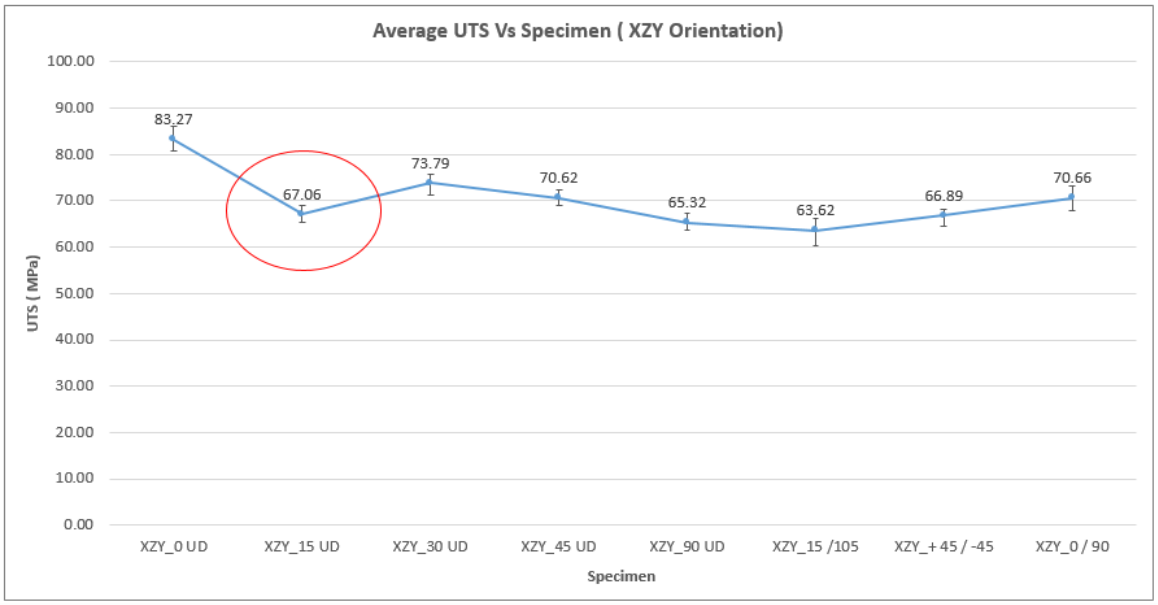

Figure 6-11 Comparison of ultimate tensile strength for different raster orientations along XZY plane

All broken specimens of 15°,30° and 45° unidirectional raster orientation specimens were investigated and after complete cross check of results for every specimen it was clear that all specimen with 15° raster orientation was showing pretty less strength as compared to 30° and 45° unidirectional specimen. Figure 6.12 gives clear idea of the uncommon behavior of every 15° raster oriented specimen. Similar behavior can observed in the case of 15° /105° alternate case as it shows less strength than 90° unidirectional specimen.

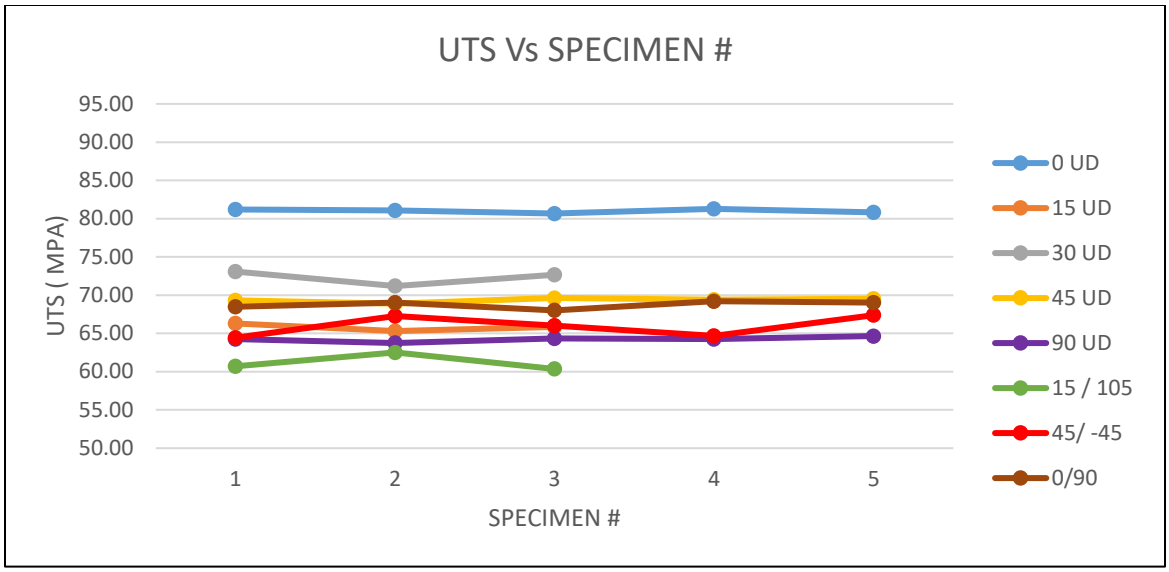

Figure 6-12 Graphical comparison of ultimate tensile strength for each specimen of different raster orientation along XZY plane

In detail comparison of cross section of each specimen helped to understand the irregular behavior of 15° raster oriented specimen. Figure 6.13 presents the cross section of each specimen. It is very clear that because of geometric differences there are some extra void places in the case of 15° raster oriented specimen. The dimension of void spaces in 30° and 45° specimen is pretty short as compared to 15° oriented specimen. Therefore it becomes the main reason to create the stress concentration resulting in easier break of the specimen.

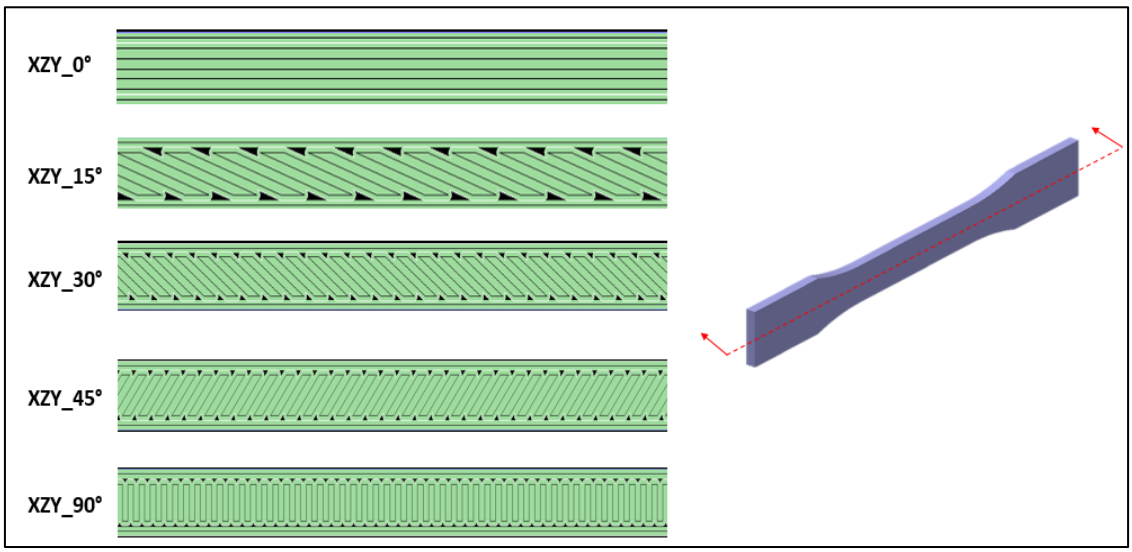

Figure 6-13 Cross section comparison for all raster orientations along XZY plane

4) ZXY Plane:

Summary of the tension test results for different raster orientations in ZXY plane are graphically shown in Fig. 6.14. The mean ultimate strength was largest for the 45° raster orientation, 40.73 MPa and weakest for the alternate layered 0° / 90° raster orientation, 27.91 MPa. Even though this are average numbers, it can been seen that error bar shows big fluctuation in this case. Therefore it is necessary to investigate each iteration of all raster orientations.

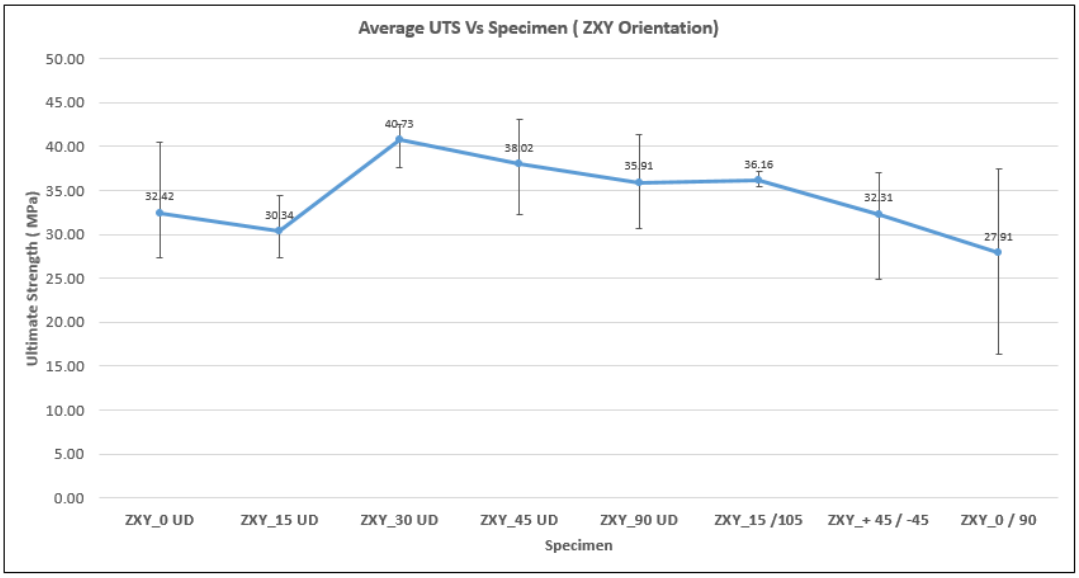

Figure 6-14 Comparison of ultimate tensile strength for different raster orientations along ZXY plane

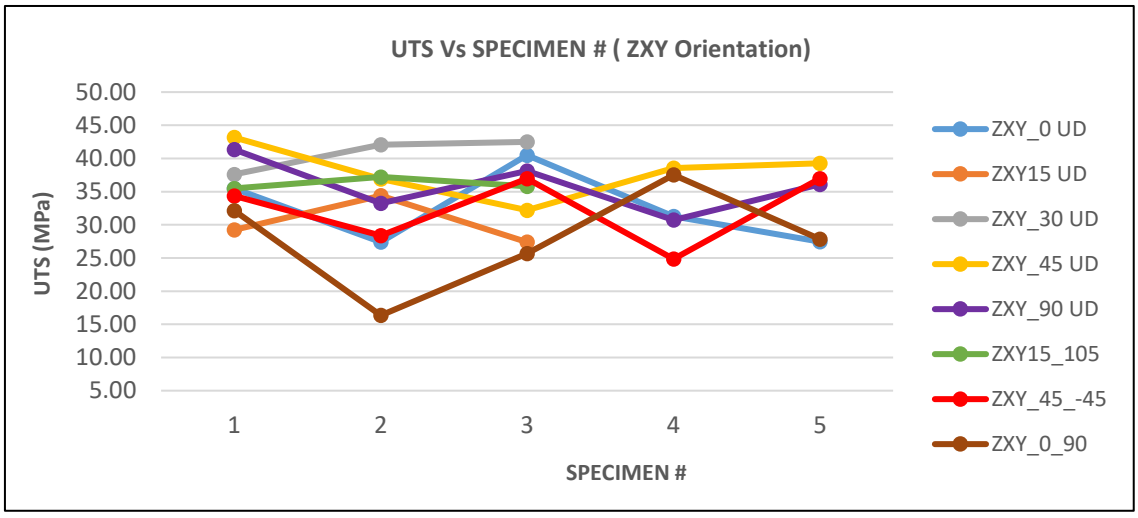

Figure 6-15 Graphical comparison of ultimate tensile strength for each specimen of different raster orientation along XZY plane

Figure 6.15 shows the variation of all specimens with different raster orientations along ZXY plane. It is observed that there is no consistency in any specimens with particular raster orientation. All specimen approximately varies from 20 MPa to 45 MPa. Therefore from this results it is difficult to decide which raster orientation presents highest strength. And for the same reason calculation of mean ultimate strength should not help to get the conclusion for different orientations in ZXY plane. But it is very important to understand the reason for this kind of variation. Therefore all specimens were investigated to check the failure patterns and cross sections of every broken specimen as shown below,

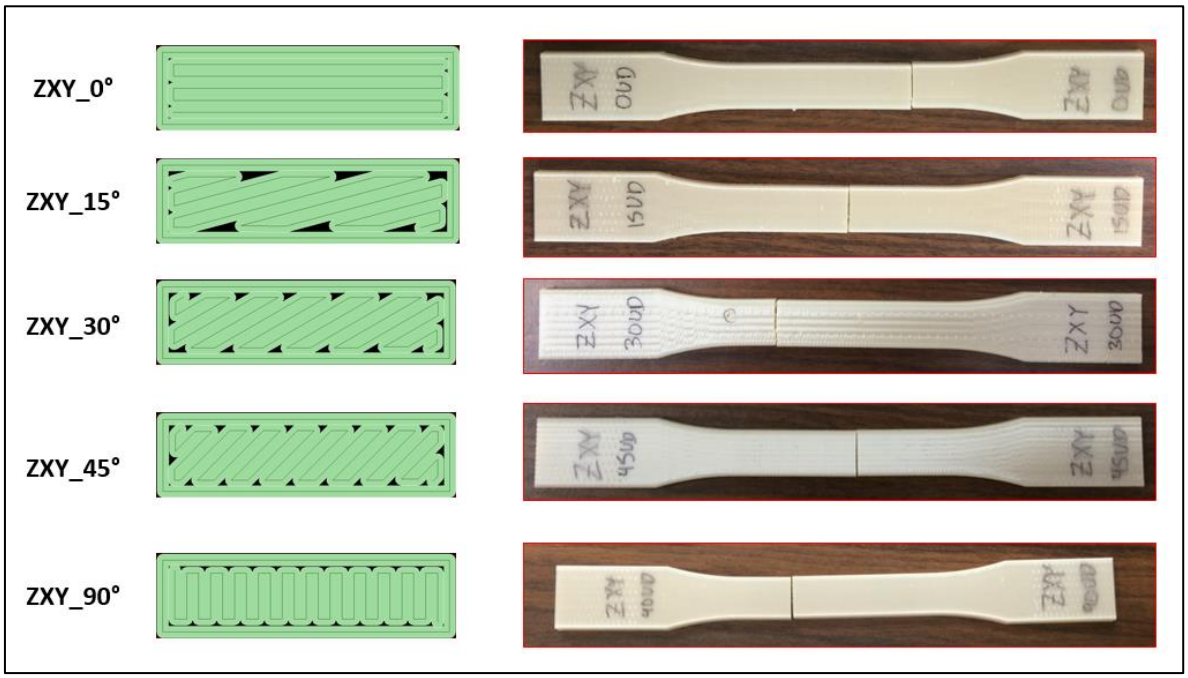

Figure 6-16 Cross Section and Failure pattern of 0°, 15°, 30°, 45° and 90° oriented specimen

In this case, even though cross section of 15° oriented specimen has highest void spaces, it is not making much difference in the final ultimate strength of the specimen. But when we check the failure pattern of each specimen it is clear that specimen fails in the same manner along the transverse direction of applied load. Failure pattern is exactly similar for all specimens as they all fail because of delamination instead of fracture. After clear inspection of each specimen it was clear that none of the specimen broke through the material but they just get delaminated along the Z-axis. Therefore impact of delamination is more in the case of ZXY plane orientation which causes the variations in final ultimate strength of specimens.

6.4.2 Short Beam Shear Test :

1) XYZ Plane:

Summary of the shear test results for different raster orientations in XYZ plane are graphically shown in Fig. 6.17. The mean shear strength was largest for the 0° raster orientation, 18.06 MPa and weakest for the alternate layered 0° / 90° raster orientation, 13.89 MPa.

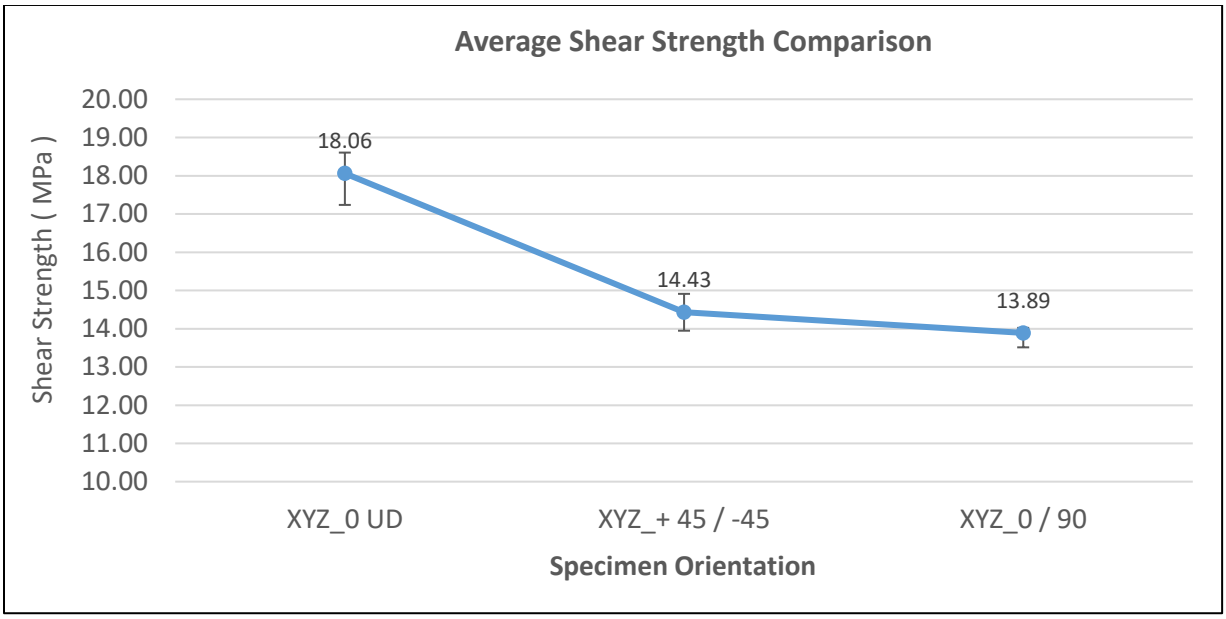

Figure 6-17 Graphical comparison of shear strength for different raster orientations along XYZ plane

We can see that unidirectional specimen represents more shear strength as compared to the specimen with alternate layers. But in this case, effect of 0° raster orientation could be the major factor rather than unidirectional layers. Behavior of short beam along different unidirectional orientations might provide clear picture of orientation effect. Specimen with alternate 0°/90° layers shows least strength and the specimen with alternate +45°/-45° layers is just little bit stronger than 0°/90° because layers along 0° holds the best strength but the layers along 90° easily try to get delaminated along force direction which indirectly brings strongest and weakest layers together giving intermediate results.

Also it is observed that 0° specimen did not break under maximum loading conditions whereas specimen with alternate +45°/-45° layers and 0°/90° breaks along the crisscross pattern at the center.

2) XZY Plane:

Summary of the shear test results for different raster orientations in XYZ plane are graphically shown in Fig. 6.18. The mean shear strength was largest for the 0° raster orientation, 18.06 MPa and weakest for the alternate layered 0° / 90° raster orientation, 13.89 MPa.

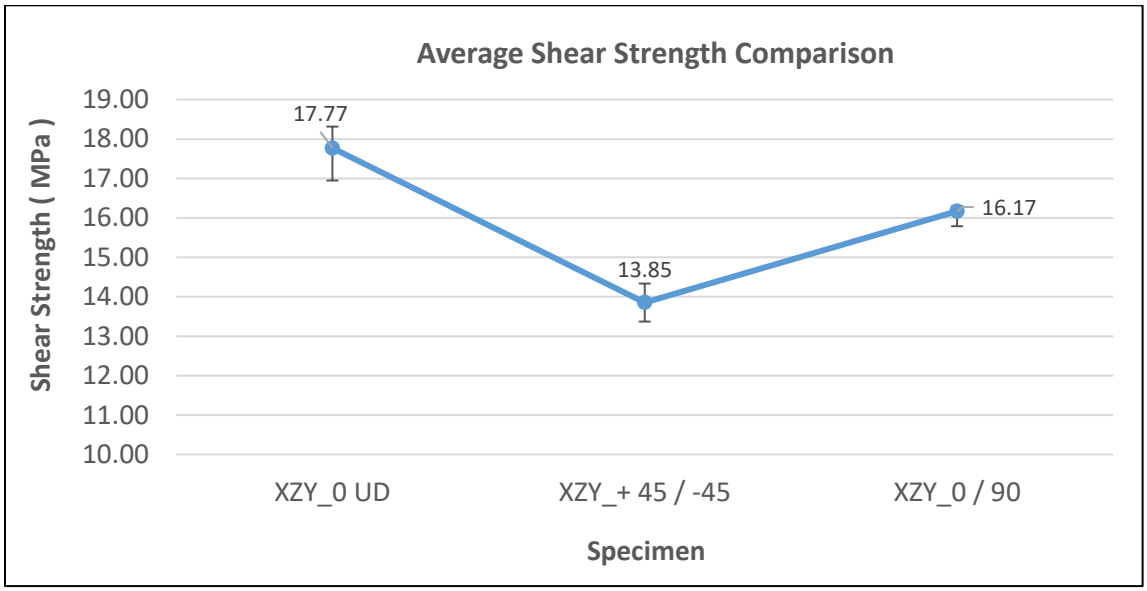

Figure 6-18 Graphical comparison of shear strength for different raster orientations along XZY plane

Specimen with 0°/90° alternating layers shows pretty close results to 0° unidirectional specimen which pulls attention towards the length of 90° oriented layers. As 90° oriented layers has shorter lengths the impact of 0° layers get higher as compared to 90° specimen therefore it provides higher resistance to bending force resulting in higher shear strength as compared to XYZ plane. Specimen with alternate +45°/-45° layers shows least strength with very consistent results similar as in XYZ plane. It is also observed that 0° specimen did not break under maximum loading conditions whereas specimen with alternate +45°/-45° layers and 0°/90° breaks catastrophically along the crisscross pattern at the center as shown in figure below,

Figure 6-19 Break pattern of 0°, +45°/-45° and 0°/90° specimen under shear test

3) ZXY Plane:

Summary of the shear test results for different raster orientations in XYZ plane are graphically shown in Fig. 6.20. The mean shear strength was largest for the 0° raster orientation, 11.86 MPa and weakest for the alternate layered +45°/-45° raster orientation, 10.40 MPa. But overall all shear strengths are very close to each other.

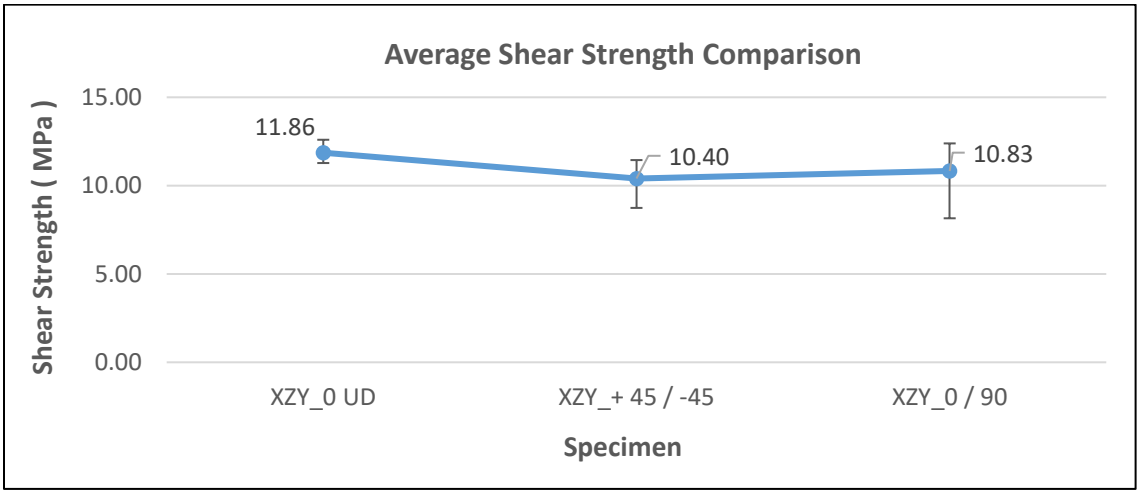

Figure 6-20 Comparison of shear strength for different raster orientations along XZY plane

It is observed that shear strength for different orientations is almost similar and it did not make any difference with change in raster orientations as all breaking took place through delamination between layers. After evaluation of all specimen results it was clear that for every type of raster orientation fluctuations were observed in the shear strengths because of which it is difficult to decide which orientation shows the best results.

Investigation of broken specimen gave clear picture of the delamination along the layers. Broken specimen showed up with very smooth cross section and clear raster pattern can be observed by naked eyes as shown below,

Figure 6-21 Broken cross section of 0°, +45°/-45° and 0°/90° oriented specimen

6.4.3 Iosipescu Test :

1) XYZ Plane:

Summary of the shear test results for different raster orientations in XYZ plane are graphically shown in Fig. 6.22. The mean shear strength was largest for the +45°/-45° raster orientation, 43.79 MPa and weakest for the unidirectional 90° raster orientation, 19.27 MPa. There is big difference observed in strengths of +45°/-45° and 0° specimen.

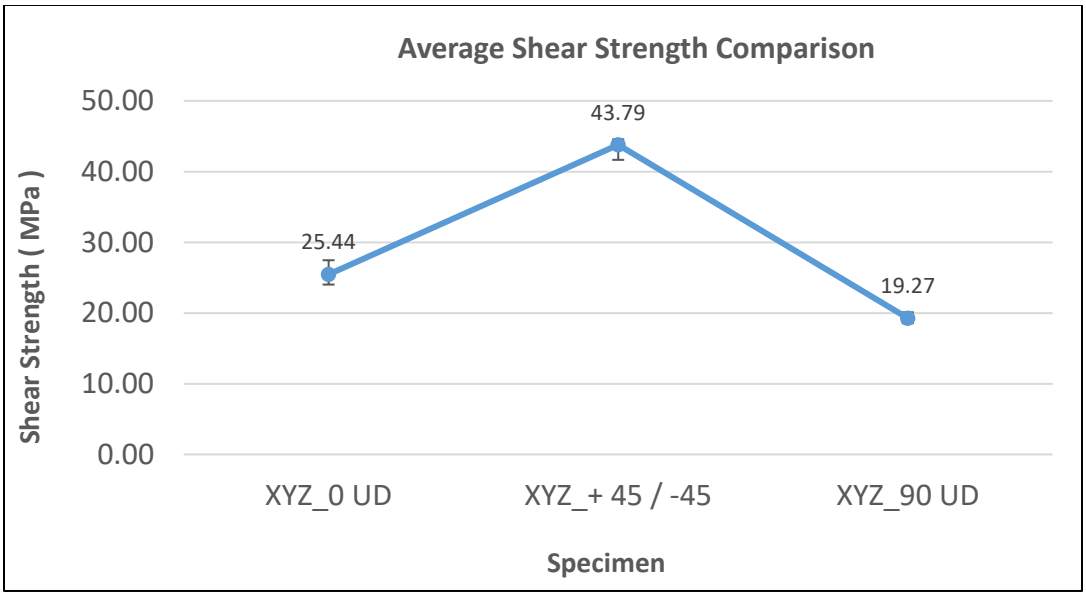

Figure 6-22 Graphical comparison of shear strength for different raster orientations along XZY plane

Investigation of tested samples shows that specimen oriented along 0° did not break neither any crack or signs of fracture are observed in specimen. But clear shear effect can be seen along the length of the fibers. Even though specimen did not break but still the shear strength along 0° shows poor results may be because of the void spaces available at the bottom of the V-notch area of 0° specimen as shown below,

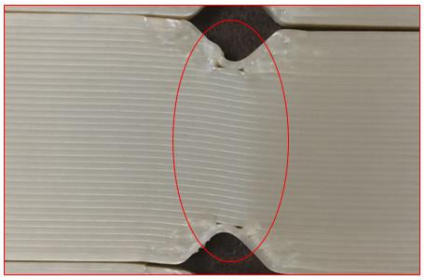

Figure 6-23 Void spaces in 0° raster oriented specimen along XYZ plane

On the other side, symmetric and consistent break pattern has been observed along +45°/-45° and 90° raster orientations. All specimens broke very perfectly along the layer pattern as shown below,

Figure 6.24. Fracture pattern of +45°/-45° and 90° raster oriented specimen

2) XZY Plane:

Summary of the shear test results for different raster orientations in XZY plane are graphically shown in Fig. 6.25. The mean shear strength was largest for the +45°/-45° raster orientation, 42.06 MPa and weakest for the unidirectional 90° raster orientation, 40.95 MPa. But overall the difference among all orientation is negligible. All strengths are pretty close to each other and does not vary much with change in the raster orientation. So we can say that raster orientation does not have much impact on shear strength.

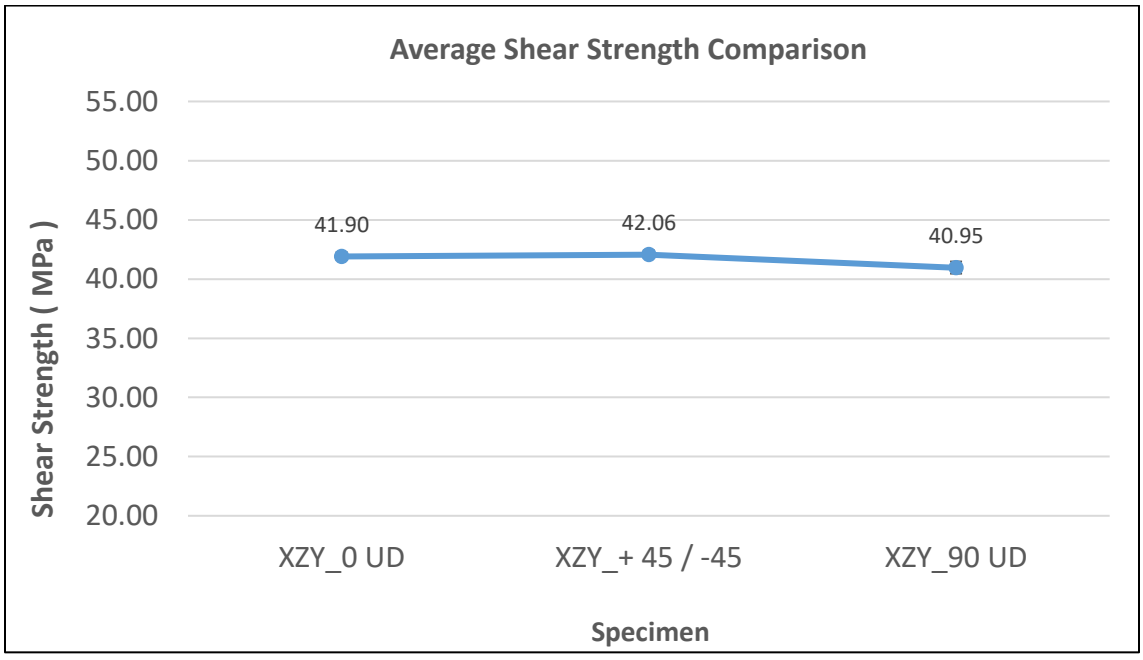

Figure 6-25 Graphical comparison of shear strength for different raster orientations

3) ZXY Plane:

Summary of the shear test results for different raster orientations in XZY plane are graphically shown in Fig. 6.26. The mean shear strength was largest for +45°/-45° raster orientation, 40.48 MPa and weakest for the unidirectional 0° raster orientation, 35.54 MPa. The results displayed through this test are completely different as compared to all previous cases. This is the only scenario where specimen with 0° raster orientation shows the least strength.

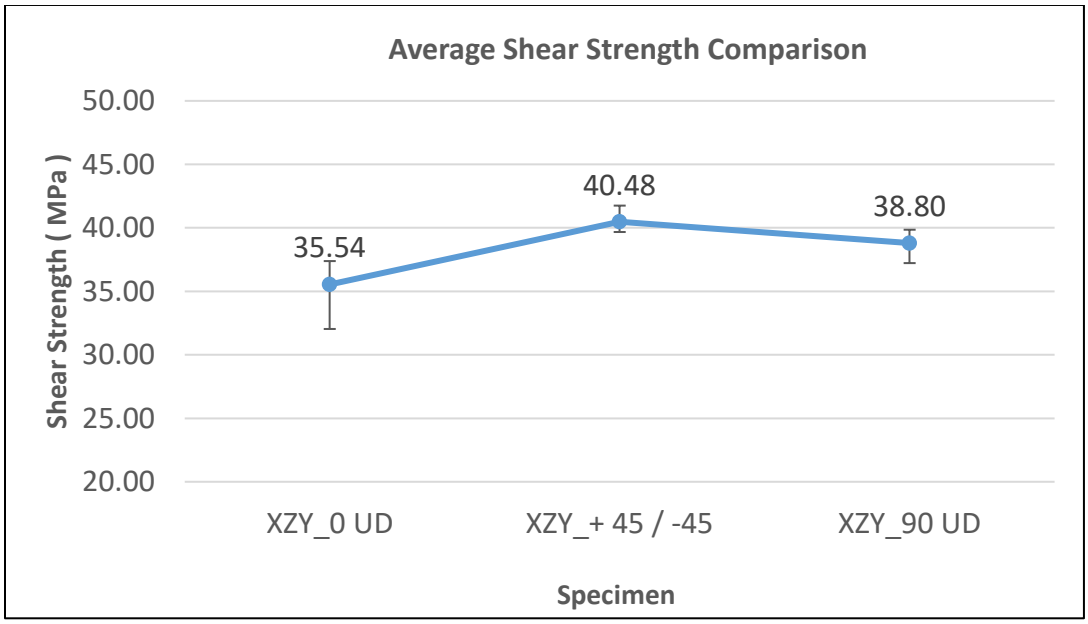

Figure 6.26. Comparison of shear strength for different raster orientations along ZXY plane

As all specimens are manufactured along the Z-axis, most of the specimen are delaminated along the V-notch. But in case of +45°/-45° there is clear picture of fracture observed passing through the V-notch. Therefore we just compared the fracture pattern of 0° and +45°/-45° specimen as shown below. This study needs further investigation.

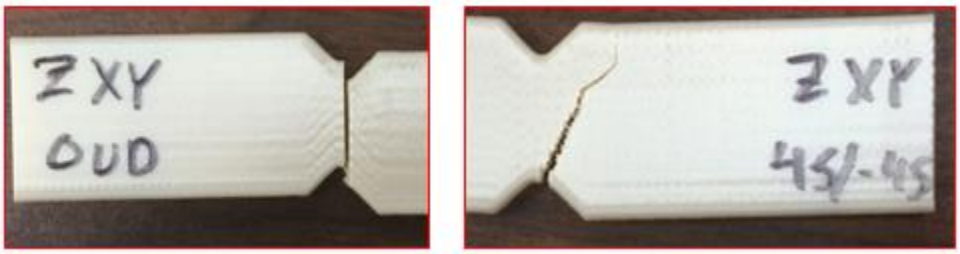

Figure 6-27 Comparison of fracture pattern along 0° and +45°/-45° specimen

6.5 CONCLUSION:

The mechanical properties of ULTEM-9085 resin specimens fabricated by fused deposition modelling display anisotropic behavior and are significantly influenced by the orientation of the layered raster's and the resulting directionality of the polymer molecules. The presence of air gaps and the quantity of air voids between the raster's and fibers additionally influences the strength and effective strength in regard to all of the tests completed in this study.

Tension tests indicate that the ultimate strengths varies along XYZ, XZY and ZXY planes. For XYZ plane ultimate strength is largest for the 0° raster orientation, followed by the 15°, 0°/90°, +45°/-45, 15°/105°,30°,45° and 90° orientations in descending order. For XZY plane ultimate tensile strength is largest for 0° raster orientation, followed by the 30°,45°,0°/90°,15°,+45°/-45°, 90° and 15°/105° in descending order. For ZXY plane ultimate strength varies as breaking takes place because of the delamination of the layers.

The differences between mean ultimate tensile strengths are significant for all pairwise comparisons of different raster orientations. Fracture paths are affected by the directionality of the polymer molecules and the strength of individual layers. The longitudinal specimens benefit from the alignment of molecules along the stress axis.

REFERENCES

[1] Ziemian, C. W., D. E. Cipoletti, S. N. Ziemian, M. N. Okwara, and K. V. Haile. "*Monotonic and Cyclic Tensile Properties of ABS Components Fabricated by Additive Manufacturing*."

[2] Sung-Hoon Ahn Michael Montero Dan Odell Shad Roundy Paul K. Wright, (2002),"*Anisotropic material properties of fused deposition modeling ABS*", Rapid Prototyping Journal, Vol. 8 Iss 4 pp. 248 - 257

[3] Q. Sun G.M. Rizvi C.T. Bellehumeur P. Gu, (2008),"Effect of processing conditions on the bonding quality of FDM polymer filaments", Rapid Prototyping Journal, Vol. 14 Iss 2 pp. 72 - 80

[4] Ziemian, Constance, Mala Sharma, and Sophia Ziemian. "*Anisotropic mechanical properties of ABS parts fabricated by fused deposition modelling*." INTECH Open Access Publisher, 2012.

[5] Huang, Bin. "Alternate slicing and deposition strategies for Fused Deposition Modelling." PhD diss., Auckland University of Technology, 2014.

[6] http://3dfabprint.com/3d-printing-ceramics-how-does-this-technology-work/

[7] http://www.maxfac.com/stereosc.html

[8] https://en.wikipedia.org/wiki/3D_printing

[9] https://hackaday.io/project/12439-fdmproperties

[10] http://my3dmatter.com/wp-content/uploads/2015/03/infillpercentimage.png

[11] http://my3dmatter.com/wp-content/uploads/2015/03/infillpatternimage.png

[12] http://my3dmatter.com/wp-content/uploads/2015/03/layerheightimage.png

[13] https://en.wikipedia.org/wiki/Stress_intensity_factor#/media/File:Fracture_modes_v2.svg

[14] https://en.wikipedia.org/wiki/Stress_intensity_factor

[15] https://en.wikipedia.org/wiki/Stress_intensity_factor#/media/File:CrackInfinitePlate.svg

[16] https://plastics.ulprospector.com/generics/1/c/t/acrylonitrile-butadiene-styrene-abs-properties-processing

[17] http://classes.engr.oregonstate.edu/mime/winter2012/me453-001/Lab1%20-%20Shear%20Strain%20on%20Polymer%20Beam/ASTM%20D638-02a.pdf

[18] https://www.astm.org/DATABASE.CART/HISTORICAL/D5379D5379M-05.htm

[19] Scheirs. J., 2000, “Compositional and failure analysis of polymers: a practical approach”. John Wiley & Sons. pp.311-315. Chap.12.

[20] OSBORN, T., E. ZHOU, R. GERZESKI, D. MOLLENHAUER, GP TANDON, TJ WHITNEY, and EV IARVE. "Experimental and Theoretical Evaluation of Stiffness Properties of Fused Deposition Modeling Parts." In *American Society of Composites-30th Technical Conference*. 2015.

[21] Ziemian, Constance, Mala Sharma, and Sophia Ziemian. *Anisotropic mechanical properties of ABS parts fabricated by fused deposition modelling*. INTECH Open Access Publisher, 2012.

[22] Fodran, Eric, Martin Koch, and Unny Menon. "Mechanical and dimensional characteristics of fused deposition modeling build styles." In *Solid Freeform Fabrication Proc*, pp. 419-442. 1996.

[23] Hutmacher, Dietmar W., Thorsten Schantz, Iwan Zein, Kee Woei Ng, Swee Hin Teoh, and Kim Cheng Tan. "Mechanical properties and cell cultural response of polycaprolactone scaffolds designed and fabricated via fused deposition modeling." *Journal of biomedical materials research* 55, no. 2 (2001): 203-216.

[24] Croccolo, Dario, Massimiliano De Agostinis, and Giorgio Olmi. "Experimental characterization and analytical modelling of the mechanical behaviour of fused deposition processed parts made of ABS-M30." *Computational Materials Science* 79 (2013): 506-518.

[25] EVans, Aw G., and E. Arn Charles. "Fracture toughness determinations by indentation." *Journal of the American Ceramic society* 59, no. 7-8 (1976): 371-372.

[26] Erdogan, Fazil. "Fracture Mechanics of Functionally Graded Materials." *MRS Bulletin* 20, no. 01 (1995): 43-44.

[27] http://my3dmatter.com/influence-infill-layer-height-pattern/

[28] http://hackaday.com/2016/02/05/filament-thickness-sensors-what-are-they-and-what-are-they-good-for/

[29] https://en.wikipedia.org/wiki/Stress_intensity_factor

BIOGRAPHICAL INFORMATION

Amit Khatri was born and raised in Maharashtra, India. He recived Bachelor’s degree from Jawaharlal Nehru College of Engineering, Maharashtra, India in August 2011. He moved to Arlington to pursue Master's degree from University of Texas, Arlington in Fall 2014. He started working on advanced techniques in 3D printing manufacturing under supervision of Dr. Ashfaq Adnan. His research focus is to understand and develop studies on mechanical behavior of 3D printed structures.